

APPLICATION OF THE FINITE ELEMENT TECHNIQUE  
TO THE THERMAL ANALYSIS OF A CONDUCTIVE MEDIUM  
SUBJECTED TO ELECTRICAL LOADING

by

Robert A. Ress, Jr.

Submitted in Partial Fulfillment of the Requirements  
for the Degree of  
Master of Science in Engineering  
in the  
Mechanical Engineering  
Program

Frank J. Tarantini March 12, 1982  
Advisor Date

Acting Sally M. Hotchkiss March 25, 1982  
Dean of the Graduate School Date

YOUNGSTOWN STATE UNIVERSITY

March, 1982

## ABSTRACT

APPLICATION OF THE FINITE ELEMENT TECHNIQUE  
TO THE THERMAL ANALYSIS OF A CONDUCTIVE MEDIUM  
SUBJECTED TO ELECTRICAL LOADING

Robert A. Ress, Jr.

Master of Science in Engineering

Youngstown State University, 1982

A procedure for evaluating the thermal response of a conductive medium subjected to electrical loading has been developed. The procedure utilizes the finite element technique for determining both the electrical and the thermal response of the medium. An intermediate Fortran program is used to calculate the localized power generated within the medium based on electric field intensities and current densities computed in the finite element electrical analysis. The localized power generated within the medium is then formatted by the Fortran program so that it may be used as heat input into the finite element thermal analysis.

The technique was applied to a simple rectangular flat plate structure and also to a complex structure representing a fusible terminal. Steady-state and transient solutions were obtained and the effect of including temperature-dependent material properties was investigated. Where applicable, mathematical and experimental analyses were performed to verify results of the finite element solutions.

## ACKNOWLEDGEMENTS

I would like to express my sincere appreciation to the General Motors Corporation for providing the opportunity and the resources required to undertake and complete this endeavor. In particular, I wish to thank my colleagues, Andrew Hallochak and Chung Suh, for their technical assistance.

Finally, I am grateful to my wife, Judith, for her continuing support and encouragement in my higher education.

## TABLE OF CONTENTS

	PAGE
ABSTRACT . . . . .	ii
ACKNOWLEDGEMENTS . . . . .	iii
TABLE OF CONTENTS . . . . .	iv
LIST OF SYMBOLS . . . . .	vi
LIST OF FIGURES . . . . .	viii
LIST OF TABLES . . . . .	x
CHAPTER	
I. INTRODUCTION . . . . .	1
II. THE FINITE ELEMENT METHOD . . . . .	4
III. ELECTRICAL CONDUCTION — HEAT CONDUCTION ANALOGY . . . . .	7
IV. ANALYTICAL PROCEDURE . . . . .	10
4.1 Introduction . . . . .	10
4.2 Intermediate Fortran Program . . . . .	12
4.3 Steady-State Analysis . . . . .	21
4.4 Transient Analysis . . . . .	22
4.5 Analysis With Temperature-Dependent Material Properties . . . . .	23
V. STEADY-STATE ANALYSIS OF A RECTANGULAR STRIP . . . . .	25
5.1 Introduction . . . . .	25
5.2 Finite Element Electrical Analysis . . . . .	25
5.3 Mathematical Electrical Analysis . . . . .	27
5.4 Finite Element Thermal Analysis . . . . .	33
5.5 Mathematical Thermal Analysis . . . . .	33
VI. TRANSIENT ANALYSIS OF A RECTANGULAR STRIP . . . . .	38

6.1	Introduction . . . . .	38
6.2	Finite Element Thermal Analysis . . .	39
6.3	Mathematical Thermal Analysis . . . .	39
VII.	STEADY-STATE ANALYSIS OF A RECTANGULAR STRIP WITH TEMPERATURE-DEPENDENT MATERIAL PROPERTIES . . . . .	45
7.1	Introduction . . . . .	45
7.2	Analytical Results . . . . .	45
VIII.	STEADY-STATE ANALYSIS OF A FUSIBLE TERMINAL .	50
8.1	Introduction . . . . .	50
8.2	Experimental Temperature Survey . . .	50
8.3	Finite Element Electrical Analysis . .	55
8.4	Finite Element Thermal Analysis . . .	60
IX.	CONCLUSIONS AND DISCUSSION . . . . .	67
9.1	Conclusions . . . . .	67
9.2	Discussion . . . . .	68
APPENDIX	Material Properties . . . . .	72
BIBLIOGRAPHY	. . . . .	76
REFERENCES	. . . . .	77

## LIST OF SYMBOLS

SYMBOL	DEFINITION	UNIT
$c$	Specific heat	Joule/kg- $^{\circ}$ C
$C, C_1, C_2$	Constants of integration	
$\bar{E}$	Electric field intensity	volt/mm
$E_x, E_y, E_z$	Components of electric field intensity in x, y, z directions, respectively	volt/mm
$\bar{i}, \bar{j}, \bar{k}$	Unit vectors in x, y, z directions, respectively	
$\bar{I}$	Current	Ampere
$\bar{J}$	Current density	Ampere/mm <sup>2</sup>
$J_x, J_y, J_z$	Components of current density in x, y, z directions, respectively	Ampere/mm <sup>2</sup>
$K$	Thermal conductivity	Watt/mm- $^{\circ}$ C
$L$	Length	mm
$P$	Power generated per unit volume	Watt/mm <sup>3</sup>
$q$	Heat generated per unit volume	Watt/mm <sup>3</sup>
$s$	Area	mm <sup>2</sup>
$t$	Time	sec
$T$	Temperature	$^{\circ}$ C
$T_w$	Temperature at wall	$^{\circ}$ C
$x, y, z$	Space coordinates in Cartesian system	
$\alpha$	Thermal diffusivity	mm <sup>2</sup> /sec
$\theta$	Temperature difference, $T - T_{\text{reference}}$	$^{\circ}$ C

SYMBOL	DEFINITION	UNIT
$\rho$	Density	kg/mm <sup>3</sup>
$\rho_e$	Charge density	Coulomb/mm <sup>3</sup>
$\sigma$	Electrical conductivity	mho/mm
$\phi$	Voltage	volt
$\nabla$	Del operator	

## LIST OF FIGURES

FIGURE	PAGE
1. Fusible Terminal . . . . .	1
2. Basic Flow Diagram of Analytical Procedure . .	11
3. Electrical Program Listing With Intermediate Fortran Program Call Up . . . . .	13
4. Electrical Program Listing With Intermediate Fortran Program Call Up, Continued . . . . .	14
5. Thermal Program Listing . . . . .	15
6. Thermal Program Listing, Continued . . . . .	16
7. Flow Diagram of Intermediate Fortran Program .	17
8. Intermediate Fortran Program Listing . . . . .	18
9. Intermediate Fortran Program Listing, Continued . . . . .	19
10. MSC/NASTRAN Volume Heat Addition Card . . . . .	21
11. Heat Input File Listing . . . . .	22
12. Flow Diagram of Analytical Procedure For an Analysis Including Temperature-Dependent Material Properties . . . . .	24
13. Finite Element Model of Rectangular Strip . . .	26
14. Temperature Isotherms — Steady-State Analysis . . . . .	35
15. Curve of Current vs. Time For Transient Analysis . . . . .	38
16. Transient Temperature Output . . . . .	40
17. Temperature Measurement Locations . . . . .	52
18. Schematic of Experimental Test Set-Up . . . . .	53
19. Experimental Test Set-Up . . . . .	54
20. Fusible Terminal Finite Element Model — Solid Elements . . . . .	57



FIGURE	PAGE
21. Fusible Terminal Finite Element Model — Plate Elements . . . . .	58
22. Equipotential Lines — Fusible Terminal . . . . .	61
23. Temperature Isotherms — Fusible Terminal . . . . .	62
24. Grid Point Locations For Thermal Output . . . . .	64
25. Grid Point Locations For Thermal Output . . . . .	65
26. Curve of Current vs. Time For Fusible Terminal Protecting Three Meters of 12 Gage Cable . . . . .	69
27. Flow Diagram of Analytical Procedure With Automated Time Step Solution Technique . . . . .	70
28. Curve of Electrical Conductivity vs. Temperature For SAE 1010 Steel . . . . .	74
29. Curve of Thermal Conductivity vs. Temperature For SAE 1010 Steel . . . . .	75

## LIST OF TABLES

TABLE	PAGE
1. Analogous Electrical and Thermal Quantities . . .	9
2. Voltage Output . . . . .	28
3. Electric Field Intensity and Current Density Output . . . . .	29
4. Heat Input Data . . . . .	29
5. Voltage Output From Mathematical Analysis . . .	32
6. Temperature Output . . . . .	34
7. Temperature Output From Mathematical Analysis .	37
8. Mathematical vs. Finite Element Results . . . .	44
9. Electrical Conductivity Per Iteration . . . . .	46
10. Iterative Temperature Output . . . . .	48
11. Maximum Temperature Per Iteration . . . . .	49
12. Results of Experimental Temperature Survey . .	56
13. Temperature Output . . . . .	63
14. Experimental vs. Analytical Results . . . . .	66
15. Material Properties . . . . .	73

## CHAPTER I

### INTRODUCTION

The fusible terminal of the type shown in Fig. 1, is used in the automotive industry to protect the main chassis wiring harness if a short circuit occurs in the unfused part of the wiring. The fusible terminal is designed to melt in the narrow portion of the terminal under a prolonged short circuit condition.



Fig. 1. Fusible Terminal

The determination of the thermal response of such a device has traditionally been accomplished through experimental blow tests and temperature surveys. Mathematical

analysis is usually not practical due to the complexity of the problem - i.e., irregular geometric configuration, time-varying electrical loading, temperature-dependent material properties, etc. As a result, the sizing of a fusible terminal for a specific application becomes a tedious and time-consuming operation.

To aid in the design of the fusible terminal, an analytical procedure for evaluating the thermal response of such a device has been developed. The procedure would apply not only to a fusible terminal but to any conductive medium subjected to electrical loading. The procedure utilizes the finite element technique for determining both the electrical and the thermal response of the medium. Although the electrical analysis capability is not directly accessible in existing finite element programs, the analogy between electrical conduction and heat conduction allows the heat transfer portion of a finite element program to be used for an electrical analysis. An intermediate Fortran program is used to calculate the localized power generated within the medium based on electric field intensities and current densities computed in the finite element electrical analysis. The localized power generated within the medium is then formatted by the Fortran program so that it may be used as heat input into the finite element thermal analysis. The temperature distribution within the medium is then determined through the finite element thermal analysis.

The technique was applied first to a simple rectangular flat plate structure. Both the steady-state and the transient response of the rectangular strip were determined. Mathematical analyses were performed to verify the finite element results of the steady-state electrical analysis, the steady-state thermal analysis and the transient thermal analysis. The solution technique necessary for the inclusion of temperature-dependent material properties was also demonstrated in a steady-state analysis of the rectangular strip.

In order to demonstrate the procedure on a large-scale problem, the technique was applied to a fusible terminal. The steady-state response of the fusible terminal was determined. An experimental temperature survey was performed to provide realistic boundary and loading conditions for the electrical and thermal analyses and also to verify the finite element results of the steady-state thermal analysis of the fusible terminal.

## CHAPTER II

## THE FINITE ELEMENT METHOD

The finite element method is a numerical procedure which was originally applied to problems of structural and solid mechanics. The recognition of the equivalence of the finite element method with a minimization process led to the application of the method to non-structural type problems. Zienkiewicz<sup>1</sup> discusses the application of the finite element method to problems governed by the Laplace and Poisson's equation - i.e., heat conduction, the lubrication of bearings, the distribution of electrical potential, etc. Brauer<sup>2</sup> applies the finite element method to the analysis of electric currents in a cathodic protection system. Over the last 20 years, the finite element method has evolved from a procedure for solving a very specialized type of problem into a general procedure capable of solving any differential equation.

The basic concept underlying the finite element method is that any continuous function can be approximated

---

<sup>1</sup>O. C. Zienkiewicz, The Finite Element Method in Engineering Science (London: McGraw-Hill Book Company, 1971), Chapter 15.

<sup>2</sup>John R. Brauer, "MSC/NASTRAN Analysis of Electric Currents in Cathodic Protection Systems," Proceedings of the MSC/NASTRAN Users Conference (Pasadena, California, March, 1979).

by a discrete model which consists of a set of piecewise continuous functions defined over a finite number of subdomains. The subdomains are called finite elements. The piecewise continuous functions are defined by using the values of the continuous function at a finite number of points in its domain. The finite number of points in the domain are called grid points.

A finite element model of a given function is constructed by dividing the domain into a number of finite elements. The finite elements are connected by common grid points where the values of the function are to be determined. Each element of the domain approximates the continuous function in that region by a polynomial expression defined using the grid point values of the continuous function. The combination of all element equations approximates the continuous function over the entire domain.

The values of the continuous function at the grid points are determined by minimizing an integral quantity associated with the physical process under consideration. For a structural problem, the strain energy of the system is minimized. This transforms the element equations into a set of algebraic equilibrium equations that can be solved for the grid point displacements.

Finite element programs make available numerous types of elements whose defining polynomial expressions range from linear to quadratic and cubic. This allows the

user to select an element whose behavior best fits the problem under consideration.

Many features of the finite element method have led to its widespread use in the engineering field. These features include the ability to mix element types in a single finite element model, the ability to model assemblies by changing material properties in a given area, and the ability to accept various types of loading conditions.



## CHAPTER III

## ELECTRICAL CONDUCTION — HEAT CONDUCTION ANALOGY

The mathematical equations representing electrical conduction and heat conduction are analogous. It is this analogy that allows the heat transfer portion of a finite element program to be used for an electrical analysis.

The basic differential equation governing the heat flow in a thermally conductive medium is<sup>3</sup>

$$\bar{\nabla} ( K \cdot \bar{\nabla} T ) + \dot{q} = \rho c \frac{\partial T}{\partial t} , \quad (3.1)$$

where  $K$  is the thermal conductivity,

$T$  is the temperature,

$\dot{q}$  is the heat generated per unit volume,

$\rho$  is the density,

$c$  is the specific heat, and

$t$  is the time.

The del operator,  $\bar{\nabla}$ , which appears in Equation (3.1) can be expressed, for Cartesian coordinates, as

$$\bar{\nabla} = \bar{i} \frac{\partial}{\partial x} + \bar{j} \frac{\partial}{\partial y} + \bar{k} \frac{\partial}{\partial z} , \quad (3.2)$$

where  $\bar{i}$ ,  $\bar{j}$ ,  $\bar{k}$  are unit vectors in the  $x$ ,  $y$ ,  $z$  directions, respectively.

---

<sup>3</sup>M. N. Ozisik, Boundary Value Problems of Heat Conduction (Scranton, Pennsylvania: International Textbook Company, 1968), p. 6.

For steady-state heat conduction, Equation (3.1) reduces to<sup>4</sup>

$$\bar{\nabla} \cdot (\mathbf{K} \cdot \bar{\nabla} T) = - \dot{q} . \quad (3.3)$$

The basic differential equation governing electric current flow in a conductive medium is<sup>5</sup>

$$\bar{\nabla} \cdot \bar{\mathbf{J}} = - \frac{\partial \rho_e}{\partial t} , \quad (3.4)$$

where  $\bar{\nabla}$  is the del operator,

$\bar{\mathbf{J}}$  is the current density,

$\rho_e$  is the charge density, and

$t$  is the time.

The current density,  $\bar{\mathbf{J}}$ , can be expressed as<sup>6</sup>

$$\bar{\mathbf{J}} = \sigma \cdot \bar{\mathbf{E}} , \quad (3.5)$$

where  $\sigma$  is the electrical conductivity, and

$\bar{\mathbf{E}}$  is the electric field intensity.

The electric field intensity,  $\bar{\mathbf{E}}$ , can be expressed as<sup>7</sup>

$$\bar{\mathbf{E}} = - \bar{\nabla} \phi , \quad (3.6)$$

where  $\phi$  is the electric potential or voltage.

Substituting Equation (3.6) into Equation (3.5) gives

$$\bar{\mathbf{J}} = - \sigma \cdot \bar{\nabla} \phi . \quad (3.7)$$

<sup>4</sup>Ozisik, p. 7.

<sup>5</sup>Roger F. Harrington, Time-Harmonic Electromagnetic Fields (New York: McGraw-Hill Book Company, 1961), p. 2.

<sup>6</sup>Harrington, p. 14.

<sup>7</sup>John D. Kraus and Keith R. Carver, Electromagnetics (Second edition: New York: McGraw-Hill Book Company, 1973), p. 33.

Substituting Equation (3.7) into Equation (3.4) gives

$$\bar{\nabla} ( \sigma \cdot \bar{\nabla} \phi ) = \frac{\partial \rho_e}{\partial t} . \quad (3.8)$$

As can be seen from the similarity of terms and operations, Equations (3.3) and (3.8) are analogous. The analogous quantities are listed in Table 1.

TABLE 1

ANALOGOUS ELECTRICAL AND THERMAL QUANTITIES

Electrical Quantity	Thermal Quantity
$\phi$ — voltage	T — temperature
$\sigma$ — electrical conductivity	K — thermal conductivity
$\frac{\partial \rho_e}{\partial t}$ — change in charge density with respect to time	- $\dot{q}$ — heat generated per unit volume
J — current density	- $( K \cdot \bar{\nabla} T )$ — heat flux
E — electric field intensity	- $\bar{\nabla} T$ — temperature gradient

## CHAPTER IV

## ANALYTICAL PROCEDURE

4.1 Introduction

The analytical procedure for determining the thermal response of a conductive medium subjected to electrical loading utilizes the finite element technique for determining both the electrical and the thermal response of the medium. An intermediate Fortran program is used to calculate the localized power generated within the medium based on electric field intensities and current densities computed in the finite element electrical analysis. The localized power generated within the medium is then formatted by the Fortran program so that it may be used as heat input into the finite element thermal analysis. The temperature distribution within the medium is then determined through the finite element thermal analysis. The analytical procedure is outlined in the flow diagram shown in Fig. 2.

The finite element program used for the electrical and thermal analyses was version 61 of the MSC/NASTRAN program. This program is developed and maintained by the MacNeal-Schwendler Corporation. MSC/NASTRAN is a proprietary version of the NASTRAN (NASA STRuctural ANalysis) program which was developed by the National Aeronautics

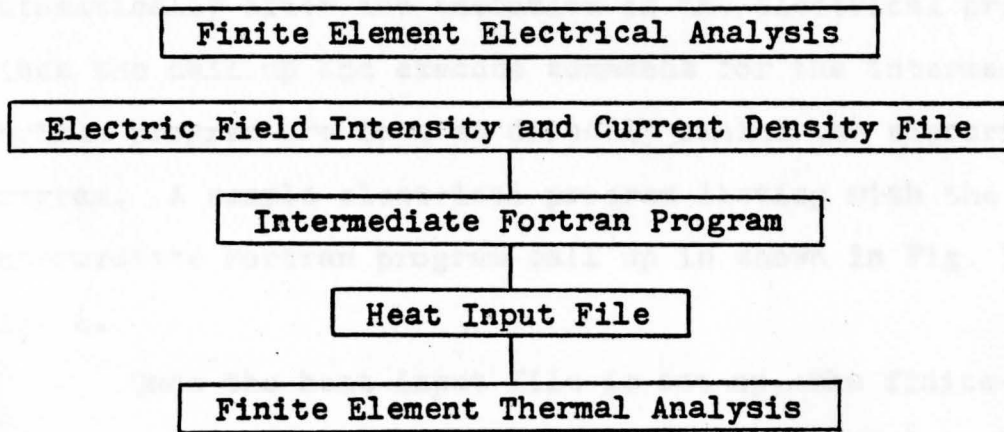


Fig. 2. Basic Flow Diagram of Analytical Procedure

and Space Administration (NASA). The advanced features of MSC/NASTRAN made it adaptable to the analytical procedure developed here.

The first step in the analytical procedure is the execution of a finite element electrical program. The electrical analysis computes the voltage at each grid point and the electric field intensity and current density at each element in the finite element model. A statement in the program causes the electric field intensities and current densities to be output to a temporary file - the electric field intensity and current density file. The temporary file is then called up by the intermediate Fortran program which calculates the power generated in each element based on information contained in the file. The intermediate Fortran program then formatts the power so that it may be used as heat input into the finite element thermal program and outputs this information to a permanent file - the heat input file. The intermediate Fortran program executes

automatically after the execution of the electrical program since the call up and execute commands for the intermediate Fortran program are located directly behind the electrical program. A sample electrical program listing with the intermediate Fortran program call up is shown in Fig. 3 and Fig. 4.

Once the heat input file is set up, the finite element thermal program may be executed. The thermal analysis uses the same finite element model that was developed for the electrical analysis. However, thermal properties are substituted for electrical properties and boundary and loading conditions are changed. A statement in the program causes the merging of the heat input file with the thermal program. The thermal analysis computes the temperature at each grid point and the temperature gradient and heat flux at each element in the finite element model. A sample thermal program listing is shown in Fig. 5 and Fig. 6.

#### 4.2 Intermediate Fortran Program

The intermediate Fortran program is used to calculate the power generated in each element of the finite element model. A flow diagram of the intermediate Fortran program is shown in Fig. 7 and a program listing is shown in Fig. 8 and Fig. 9.

The power generated in each element can be

```

//HT4PF5AA JOB (8350-1-RESS),MSGLEVEL=(1,1),MSGCLASS=T,PRTY=9
// EXEC NASTRAN,REG=700K,TIME=10,SYSOOT=X,
//      PLTCND='(0,LE,NS)'
//M.SYSIN DD *
NASTRAN BUFFSIZE=4760,HEAT=1
ID RESS,ROBERT
SOL 24
TIME 3
CEND
TITLE = FLAT PLATE, 10MM BY 40MM BY 0.81MM
SUBTITLE = LINEAR CONDUCTION CURRENT, LOAD VIA APPLIED CURRENT
LABEL = LOAD = 100 AMPS AT 10 VOLTS
ECHO=UNSORT
THERMAL=ALL
SPCFORCE=ALL
FLUX(PUNCH,PRINT)=ALLa
ESE=ALL
SPC=1
LOAD=1
OUTPUT(PLOT)
PLOTTER NASTPLT T
PAPER SIZE 13. BY 10.
SET 1 = 1 THRU 11
AXES Z,X,Y
VIEW 0.0,0.0,0.0
PTITLE = VOLTAGE CONTOURS - PLATE
FIND SCALE,ORIGIN 10,SET 1
CONTOUR MAGNIT, EVEN 11
PLOT CONTOUR,SET 1,ORIGIN 10,OUTLINE
AXES Z,X,Y
VIEW 0.0,0.0,0.0
PTITLE = FLAT PLATE
FIND SCALE,ORIGIN 11,SET 1
PLOT SET 1,ORIGIN 11,LABEL BOTH
BEGIN BULK
CQUAD4      1      1      1      3      4      2
CQUAD4      2      1      3      5      6      4
CQUAD4      3      1      5      7      8      6
CQUAD4      4      1      7      9     10      8
CQUAD4      5      1      9     11     12     10
CQUAD4      6      1     11     13     14     12
CQUAD4      7      1     13     15     16     14
CQUAD4      8      1     15     17     18     16
CQUAD4      9      1     17     19     20     18
CQUAD4     10      1     19     21     22     20
CQUAD4     11      1     23      1      2      24

```

Fig. 3. Electrical Program Listing With Intermediate Fortran Program Call Up.

<sup>a</sup>Output of electric field intensities and current densities to temporary file.

```

GRID      1      0.0      0.0      0.0
GRID      2      0.0     10.0      0.0
GRID      3      4.0      0.0      0.0
GRID      4      4.0     10.0      0.0
GRID      5      8.0      0.0      0.0
GRID      6      8.0     10.0      0.0
GRID      7     12.0      0.0      0.0
GRID      8     12.0     10.0      0.0
GRID      9     16.0      0.0      0.0
GRID     10     16.0     10.0      0.0
GRID     11     20.0      0.0      0.0
GRID     12     20.0     10.0      0.0
GRID     13     24.0      0.0      0.0
GRID     14     24.0     10.0      0.0
GRID     15     28.0      0.0      0.0
GRID     16     28.0     10.0      0.0
GRID     17     32.0      0.0      0.0
GRID     18     32.0     10.0      0.0
GRID     19     36.0      0.0      0.0
GRID     20     36.0     10.0      0.0
GRID     21     40.0      0.0      0.0
GRID     22     40.0     10.0      0.0
GRID     23     -0.0001      0.0      0.0
GRID     24     -0.0001     10.0      0.0
PQUAD4  1      1010      0.81
MAT4    1010      8333.33
SPC     1      21          10.0     22          10.0
QVOL    1      123456.8     11
ENDDATA
/*
//NS.FT07F001 DD UNIT=SYSDA,DSN=&&TEMP1,DISP=(NEW,PASS),a
// SPACE=(TRK,(20,20)),DCB=(RECFM=FB,LRECL=80,BLKSIZE=800)a
//NS.PLT2 DD SPACE=(TRK,(50,20),RLSE),
// DISP=(NEW,CATLG),DCB=(RECFM=V,BLKSIZE=3008),
// UNIT=SYSDA,DSN=HT4PF5.PLATEEL.NASTPLOT
/*
// EXEC FHCLGb
//C.SYSIN DD UNIT=SYSDA,DISP=SHR,DSN=HT4PF5.ETIMESJ.FORTb
//G.FT01F001 DD UNIT=SYSDA,DSN=&&TEMP1,DISP=(OLD,DELETE)c
//G.FT02F001 DD UNIT=SYSDA,SPACE=(TRK,(70)),DISP=SHR,d
// DCB=(RECFM=FB,LRECL=80,BLKSIZE=800),DSN=HT4PF5.ETIMESJ.DATAd
//G.FT03F001 DD UNIT=SYSDA,SPACE=(TRK,(1)),DISP=(NEW,DELETE),
// DCB=(RECFM=FB,LRECL=80,BLKSIZE=80),DSN=&&TERM2

```

Fig. 4. Electrical Program Listing With Intermediate Fortran Program Call Up, Continued.

<sup>a</sup>Set up of temporary file.

<sup>b</sup>Execution of intermediate Fortran program.

<sup>c</sup>Call up of temporary file.

<sup>d</sup>Set up of heat input file.



```

//HT4PF5AA JOB (8350-1-RESS),MSGLEVEL=(1,1),MSGCLASS=T,PRTY=9
// EXEC NASTRAN,REG=700K,TIME=10,SYSOUT=X,
//      PLTCND='(0,LE,NS)'a
//M.FT02F001 DD UNIT=SYSDA,DISP=SHR,DSN=HT4PF5.ETIMESJ.DATAa
//M.SYSIN DD *
NASTRAN BUFFSIZE=4760,HEAT=1
ID RESS,ROBERT
SOL 24
TIME 3
CEND
TITLE = FLAT PLATE, 10MM BY 40MM BY 0.81MM
SUBTITLE = LINEAR HEAT CONDUCTION, LOAD VIA VOLUME HEAT ADDITION
LABEL = LOAD = 0.01829 WATTS/MM**3
ECHO=UNSORT
THERMAL=ALL
SPCFORCE=ALL
FLUX=ALL
ESE=ALL
SPC=1
LOAD=1
OUTPUT (PLOT)
PLOTTER NASTPLT T
PAPER SIZE 13. BY 10.
SET 1 = 1 THRU 11
AXES Z,X,Y
VIEW 0.0,0.0,0.0
PTITLE = TEMPERATURE CONTOURS - PLATE
FIND SCALE,ORIGIN 10,SET 1
CONTOUR MAGNIT, EVEN 11
PLOT CONTOUR,SET 1,ORIGIN 10,OUTLINE
AXES Z,X,Y
VIEW 0.0,0.0,0.0
PTITLE = FLAT PLATE
FIND SCALE,ORIGIN 11,SET 1
PLOT SET 1,ORIGIN 11,LABEL BOTH
BEGIN BULK
CQUAD4      1      1      1      3      4      2
CQUAD4      2      1      3      5      6      4
CQUAD4      3      1      5      7      8      6
CQUAD4      4      1      7      9     10      8

```

Fig. 5. Thermal Program Listing

<sup>a</sup>Call up of heat input file.

```

CQUAD4      5      1      9      11      12      10
CQUAD4      6      1      11     13      14      12
CQUAD4      7      1      13     15      16      14
CQUAD4      8      1      15     17      18      16
CQUAD4      9      1      17     19      20      18
CQUAD4     10      1      19     21      22      20
CQUAD4     11      1      23      1      2      24
GRID        1          0.0     0.0     0.0
GRID        2          0.0    10.0     0.0
GRID        3          4.0     0.0     0.0
GRID        4          4.0    10.0     0.0
GRID        5          8.0     0.0     0.0
GRID        6          8.0    10.0     0.0
GRID        7         12.0     0.0     0.0
GRID        8         12.0    10.0     0.0
GRID        9         16.0     0.0     0.0
GRID       10         16.0    10.0     0.0
GRID       11         20.0     0.0     0.0
GRID       12         20.0    10.0     0.0
GRID       13         24.0     0.0     0.0
GRID       14         24.0    10.0     0.0
GRID       15         28.0     0.0     0.0
GRID       16         28.0    10.0     0.0
GRID       17         32.0     0.0     0.0
GRID       18         32.0    10.0     0.0
GRID       19         36.0     0.0     0.0
GRID       20         36.0    10.0     0.0
GRID       21         40.0     0.0     0.0
GRID       22         40.0    10.0     0.0
GRID       23         - .0001  0.0     0.0
GRID       24         - .0001  10.0    0.0
PQUAD4     1      1010     0.81
MAT4      1010     0.043
SPC        1      1          23.0     2      23.0
SPC        1      21         23.0     22     23.0
$MERGEa
ENDDATA
//NS.PLT2 DD SPACE=(TRK,(50,20),RLSE),
// DISP=(NEW,CATLG),DCB=(RECFM=V,BLKSIZE=3008),
// UNIT=SYSDA,DSN=HT4PF5.PLATETH.NASTPLOT

```

Fig. 6. Thermal Program Listing, Continued

<sup>a</sup>Merging of heat input file.

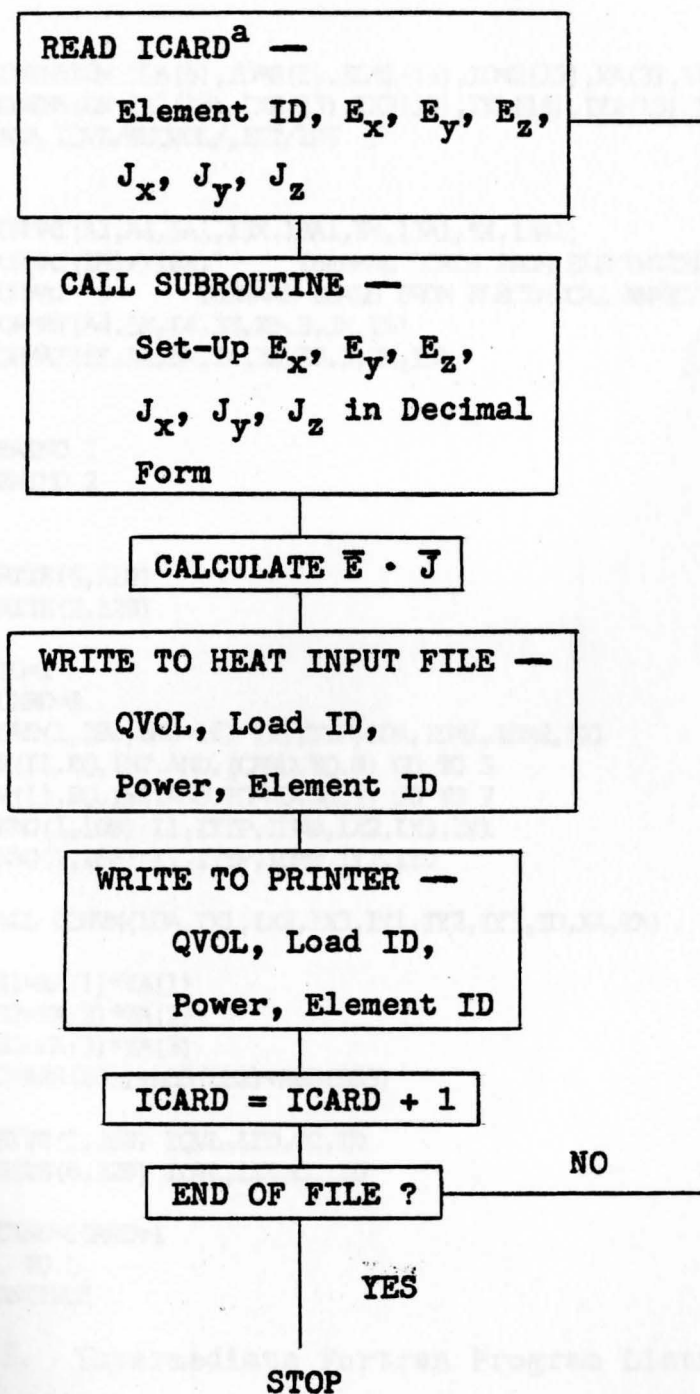


Fig. 7. Flow Diagram of Intermediate Fortran Program

<sup>a</sup>ICARD is a line of data from the temporary file.

```

00100 C
00200 C
00300     DIMENSION IDA(5),IDM0(5),IDM1(13),IDM2(13),XA(3),YA(3)
00400     DIMENSION IX1(13),IX2(13),IX3(13),IY1(13),IY2(13),IY3(13)
00500     DATA IQVL/4HQVOL/,IST/1HS /
00600 C
00700 C
00800     100 FORMAT(A1,A4,5A1,13X,13A1,5X,13A1,5X,13A1)
00900     110 FORMAT(1H1//10X,'      THERMAL LOADS FROM ELECTRICAL ANALYSIS ')
01000     120 FORMAT('$      THERMAL LOADS FROM ELECTRICAL ANALYSIS ')
01100     200 FORMAT(A4,5X,I4,3X,E8.3,3X,I5)
01200     220 FORMAT(5X,A4,5X,I4,3X,E8.3,3X,I5)
01300 C
01400 C
01500     REWIND 1
01600     REWIND 2
01700 C
01800 C
01900     WRITE(6,110)
02000     WRITE(2,120)
02100 C
02200     LID=1
02300     ICARD=0
02400     5 READ(1,100,END=10) I1,ITYP,IDA,IDM1,IDM2,IX1
02500     IF(I1.EQ.IST.AND.ICARD.EQ.0) GO TO 5
02600     IF(I1.EQ.IST.AND.ICARD.GE.1) GO TO 7
02700     READ(1,100) I1,ITYP,IDM0,IX2,IX3,IY1
02800     READ(1,100) I1,ITYP,IDM0,IY2,IY3
02900 C
03000     CALL CONVM(IDA,IX1,IX2,IX3,IY1,IY2,IY3,ID,XA,YA)
03100 C
03200     SS1=XA(1)*YA(1)
03300     SS2=XA(2)*YA(2)
03400     SS3=XA(3)*YA(3)
03500     CC=ABS(SS1)+ABS(SS2)+ABS(SS3)
03600 C
03700     WRITE(2,200) IQVL,LID,CC,ID
03800     WRITE(6,220) IQVL,LID,CC,ID
03900 C
04000     ICARD=ICARD+1
04100     GO TO 5
04200     7 CONTINUE

```

Fig. 8. Intermediate Fortran Program Listing

```

04300      GO TO 5
04400      10 CONTINUE
04500      ENDFILE 2
04600      STOP
04700      END
04800      SUBROUTINE CONVM(IDA,IX1,IX2,IX3,IY1,IY2,IY3,ID,X,Y)
04900      DIMENSION IX1(13),IX2(13),IX3(13)
05000      DIMENSION IY1(13),IY2(13),IY3(13)
05100      DIMENSION IDA(5),X(3),Y(3),Z1(6),INDX(6)
05200 C
05300 C
05400      REWIND 3
05500      WRITE(3,300) IDA
05600      WRITE(3,301) IX1,IX2,IX3,IY1,IY2,IY3
05700      300 FORMAT(5A1)
05800      301 FORMAT(6(13A1))
05900 C
06000 C
06100      REWIND 3
06200      READ(3,302) ID
06300      READ(3,303) (Z1(I),IDMY,INDX(I),I=1,6)
06400      302 FORMAT(I5)
06500      303 FORMAT(6(F9.6,A1,I3))
06600 C
06700 C
06800      M1=20
06900      DO 5 I=1,3
07000      ICH=IABS(INDX(I))
07100      ITT=INDX(I)
07200      IF(ICH.GT.M1) ITT=0
07300      XND=10.0**ITT
07400      5 X(I)=Z1(I)*XND
07500      DO 6 I=4,6
07600      ICH=IABS(INDX(I))
07700      ITT=INDX(I)
07800      IF(ICH.GT.M1) ITT=0
07900      XND=10.0**ITT
08000      6 Y(I-3)=Z1(I)*XND
08100 C
08200 C
08300      RETURN
08400      END

```

Fig. 9. Intermediate Fortran Program Listing, Continued

expressed as<sup>8</sup>

$$P = \bar{E} \cdot \bar{J} , \quad (4.1)$$

where  $P$  is the power generated per unit volume,

$\bar{E}$  is the electric field intensity at the element, and

$\bar{J}$  is the current density at the element.

$\bar{E}$  and  $\bar{J}$  are vector quantities which can be expressed as

$$\bar{E} = E_x \bar{I} + E_y \bar{J} + E_z \bar{K} , \text{ and} \quad (4.2)$$

$$\bar{J} = J_x \bar{I} + J_y \bar{J} + J_z \bar{K} , \quad (4.3)$$

where  $\bar{I}$ ,  $\bar{J}$ ,  $\bar{K}$  are unit vectors in the  $x$ ,  $y$ ,  $z$  directions, respectively,

$E_x$ ,  $E_y$ ,  $E_z$  are components of the electric field intensity in the  $x$ ,  $y$ ,  $z$  directions, respectively, and

$J_x$ ,  $J_y$ ,  $J_z$  are components of the current density in the  $x$ ,  $y$ ,  $z$  directions, respectively.

Substituting Equation (4.2) and Equation (4.3) into Equation (4.1) gives

$$P = E_x J_x + E_y J_y + E_z J_z . \quad (4.4)$$

The three components of electric field intensity and current density are computed in the electrical analysis. The intermediate Fortran program substitutes these values into Equation (4.4) and obtains the power generated in each element of the finite element model.

---

<sup>8</sup>Harrington, p. 14.

The power generated in each element must be formatted properly for input into the thermal program. The card image for the input data card which defines a rate of internal heat generation in an element is shown in Fig. 10. A volume heat addition card (QVOL) is set up by the intermediate Fortran program for each element of the finite element model and the data is stored in the heat input file for subsequent use by the thermal program. A sample heat input file is shown in Fig. 11.

#### 4.3 Steady-State Analysis

A steady-state solution is readily obtained with one pass through the analytical procedure outlined in Fig. 2. In the finite element electrical analysis, electrical loading is applied at one end of the conductive medium and a reference voltage is applied at the opposite end. In the finite element thermal analysis, fixed temperatures are ap-

	1	2	3	4
Field:	QVOL <sup>a</sup>	SID <sup>b</sup>	QV <sup>c</sup>	EID <sup>d</sup>
Sample Input:	QVOL	1	10.0	1

Fig. 10. MSC/NASTRAN Volume Heat Addition Card

<sup>a</sup>Card name.

<sup>b</sup>Load set identification number (integer).

<sup>c</sup>Power input per unit volume (real).

<sup>d</sup>Element identification number (integer).

\$ THERMAL LOADS FROM ELECTRICAL ANALYSIS			
QVOL	1	.183E-01	1
QVOL	1	.183E-01	2
QVOL	1	.183E-01	3
QVOL	1	.183E-01	4
QVOL	1	.183E-01	5
QVOL	1	.183E-01	6
QVOL	1	.183E-01	7
QVOL	1	.183E-01	8
QVOL	1	.183E-01	9
QVOL	1	.183E-01	10
QVOL	1	.457E-02	11

Fig. 11. Heat Input File Listing

plied to simulate large heat sinks. The loading for the thermal analysis comes from the heat input file.

#### 4.4 Transient Analysis

As in a steady-state solution, a transient solution where the magnitude of the electrical loading is constant is obtained with one pass through the analytical procedure outlined in Fig. 2. In the finite element electrical analysis, a steady-state electrical solution is obtained since the power generated per element will not change with time. The loading for the thermal analysis comes from the heat input file. The thermal loading is applied for a specific time period and thermal output is obtained at specified time intervals.



#### 4.5 Analysis With Temperature-Dependent Material Properties

A steady-state solution with temperature-dependent material properties requires several passes through the analytical procedure shown in Fig. 2 since the solution sequence is an iterative one. A constant value of electrical conductivity is used for the first pass through the analytical procedure. A table of thermal conductivity versus temperature is input into the thermal program where an iterative thermal solution is obtained. After each iteration, the table is used to update the thermal conductivity for each element of the finite element model and a new thermal solution is obtained. The iterative thermal solution sequence is automatic. Once the thermal solution has converged, average element temperatures are used to manually update the electrical conductivity for each element of the finite element model and the entire procedure is repeated until the electrical solution converges. The modified analytical procedure reflecting the inclusion of temperature dependent material properties is outlined in the flow diagram shown in Fig. 12.

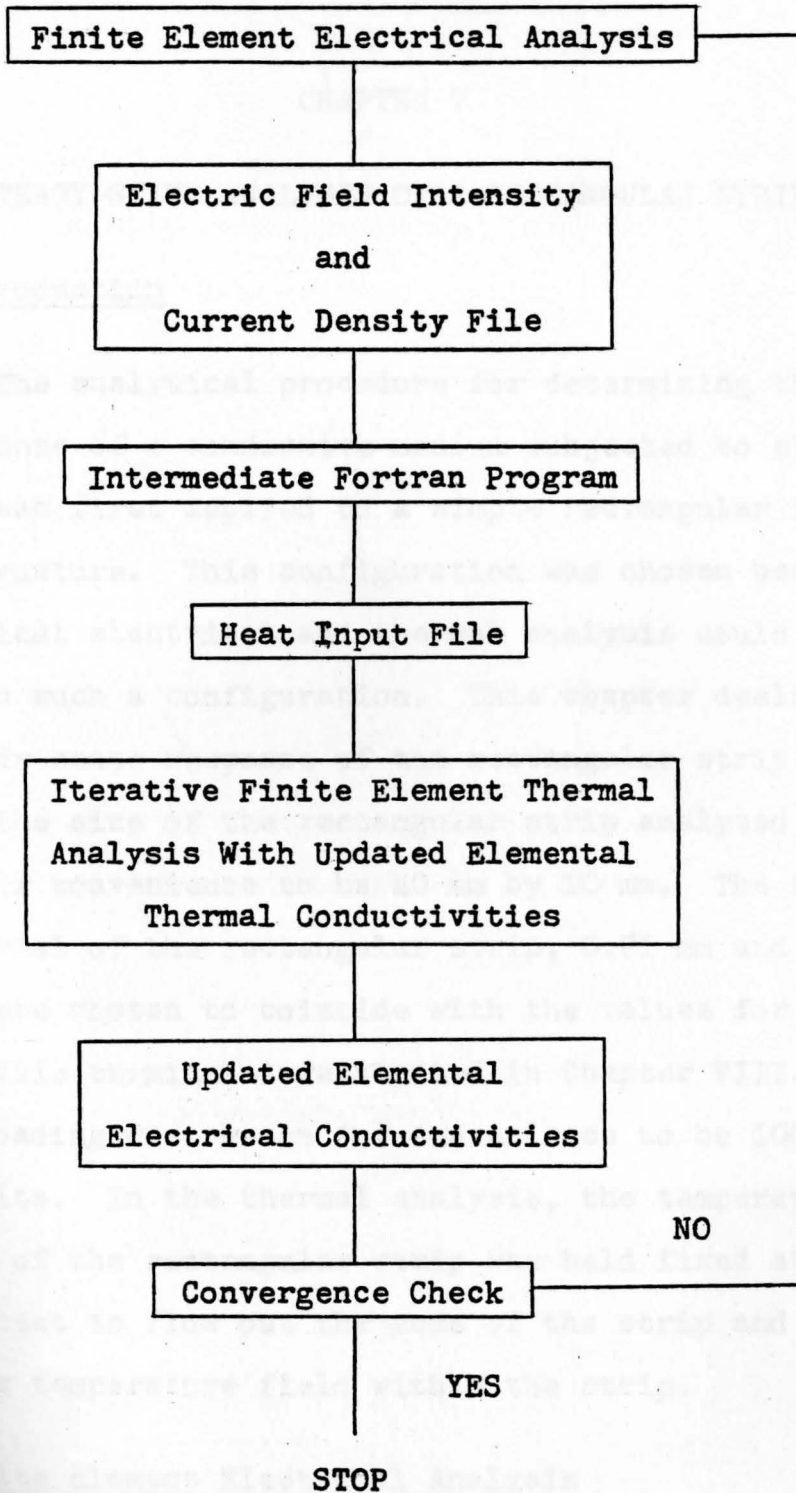


Fig. 12. Flow Diagram of Analytical Procedure For an Analysis Including Temperature-Dependent Material Properties.

## CHAPTER V

### STEADY-STATE ANALYSIS OF A RECTANGULAR STRIP

#### 5.1 Introduction

The analytical procedure for determining the thermal response of a conductive medium subjected to electrical loading was first applied to a simple rectangular flat plate structure. This configuration was chosen because a mathematical electrical and thermal analysis could be performed on such a configuration. This chapter deals with the steady-state response of the rectangular strip.

The size of the rectangular strip analyzed here was chosen for convenience to be 40 mm by 10 mm. The thickness and material of the rectangular strip, 0.81 mm and SAE 1010 steel, were chosen to coincide with the values for the actual fusible terminal investigated in Chapter VIII. Electrical loading was chosen for convenience to be 100 amperes at 10 volts. In the thermal analysis, the temperature at each end of the rectangular strip was held fixed at 23°C, causing heat to flow out the ends of the strip and creating a varying temperature field within the strip.

#### 5.2 Finite Element Electrical Analysis

The finite element model used for both the electrical and thermal analyses is shown in Fig. 13. Grid point

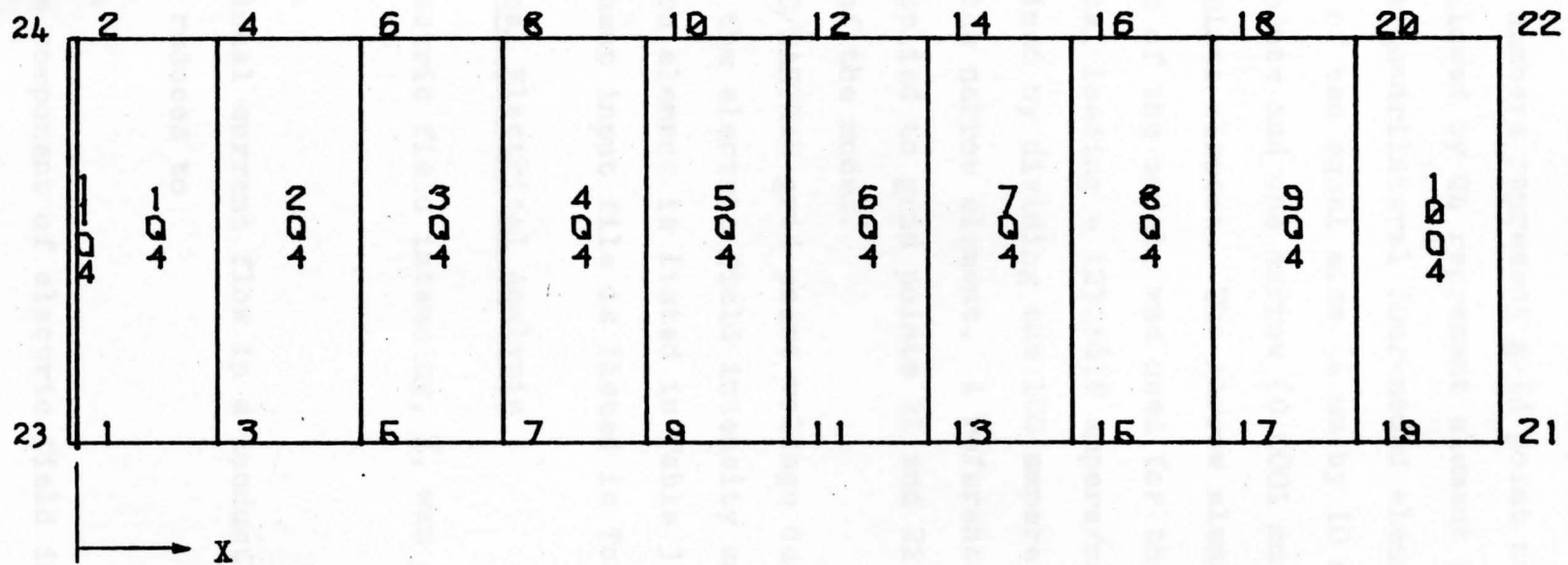


Fig. 13. Finite Element Model of Rectangular Strip

numbers and element numbers are superimposed on the model. The individual numbers represent grid point numbers, while the numbers followed by Q4 represent element numbers. The Q4 designates a quadrilateral four-noded element. The model consists of ten equal size (4 mm by 10 mm by 0.81 mm) flat plate elements and one narrow (0.0001 mm by 10 mm by 0.81 mm) flat plate element. The narrow element, located at the left end of the model, was used for the application of the electrical loading - 123456.8 ampere/mm<sup>3</sup>. This value was obtained by dividing the 100 ampere current by the volume of the narrow element. A reference voltage of 10 volts was applied to grid points 21 and 22 located at the right end of the model.

The MSC/NASTRAN grid point voltage output is listed in Table 2 and the electric field intensity and current density for each element is listed in Table 3. Data contained in the heat input file is listed in Table 4.

### 5.3 Mathematical Electrical Analysis

The electric field intensity,  $\bar{E}$ , was defined in Chapter III as

$$\bar{E} = -\bar{\nabla} \phi . \quad (3.6)$$

For one-dimensional current flow in a conductive medium, Equation (3.6) reduces to

$$E_x = -\frac{d\phi}{dx} , \quad (5.1)$$

where  $E_x$  is the component of electric field intensity in the x direction,

TABLE 2  
VOLTAGE OUTPUT

Grid Point	Axial Location <sup>a</sup> , mm	Voltage
1	0.0	10.05926
2	0.0	10.05926
3	4.0	10.05333
4	4.0	10.05333
5	8.0	10.04741
6	8.0	10.04741
7	12.0	10.04148
8	12.0	10.04148
9	16.0	10.03555
10	16.0	10.03555
11	20.0	10.02963
12	20.0	10.02963
13	24.0	10.02370
14	24.0	10.02370
15	28.0	10.01778
16	28.0	10.01778
17	32.0	10.01185
18	32.0	10.01185
19	36.0	10.00593
20	36.0	10.00593
21	40.0	10.00000
22	40.0	10.00000
23	-0.0001	10.05926
24	-0.0001	10.05926

<sup>a</sup>See Fig. 13.

TABLE 3  
ELECTRIC FIELD INTENSITY AND CURRENT DENSITY OUTPUT

Element	$E_x$ , Volt/mm	$J_x$ , Ampere/mm <sup>2</sup>
1	$1.4815 \times 10^{-3}$	12.3457
2	$1.4815 \times 10^{-3}$	12.3457
3	$1.4815 \times 10^{-3}$	12.3457
4	$1.4815 \times 10^{-3}$	12.3457
5	$1.4815 \times 10^{-3}$	12.3457
6	$1.4815 \times 10^{-3}$	12.3457
7	$1.4815 \times 10^{-3}$	12.3457
8	$1.4815 \times 10^{-3}$	12.3457
9	$1.4815 \times 10^{-3}$	12.3457
10	$1.4815 \times 10^{-3}$	12.3457
11	$7.4074 \times 10^{-4}$	6.1728

TABLE 4  
HEAT INPUT DATA

Element	Heat Input, Watt/mm <sup>3</sup>
1	$0.183 \times 10^{-1}$
2	$0.183 \times 10^{-1}$
3	$0.183 \times 10^{-1}$
4	$0.183 \times 10^{-1}$
5	$0.183 \times 10^{-1}$
6	$0.183 \times 10^{-1}$
7	$0.183 \times 10^{-1}$
8	$0.183 \times 10^{-1}$
9	$0.183 \times 10^{-1}$
10	$0.183 \times 10^{-1}$
11	$0.457 \times 10^{-2}$

$\phi$  is the voltage, and

$x$  is the axial position.

Separating variables in Equation (5.1) gives

$$E_x dx = - d\phi . \quad (5.2)$$

Integrating Equation (5.2) gives

$$E_x x = - \phi + C , \quad (5.3)$$

where  $C$  is a constant of integration.

Rearranging Equation (5.3) gives

$$\phi = - E_x x + C . \quad (5.4)$$

The current density,  $\bar{J}$ , was defined in Chapter III as

$$\bar{J} = \sigma \cdot \bar{E} . \quad (3.5)$$

For one-dimensional current flow in a conductive medium, Equation (3.5) reduces to

$$J_x = \sigma \cdot E_x , \quad (5.5)$$

where  $J_x$  is the component of current density in the  $x$  direction,

$E_x$  is the component of electric field intensity in the  $x$  direction, and

$\sigma$  is the electrical conductivity.

Rearranging Equation (5.5) gives

$$E_x = \frac{J_x}{\sigma} . \quad (5.6)$$

The current density can be expressed as<sup>9</sup>

---

<sup>9</sup>Kraus and Carver, p. 118.



$$J_x = \frac{I}{s}, \quad (5.7)$$

where  $I$  is the current, and

$s$  is the cross sectional area.

For the rectangular strip described in Section 5.1,

$$I = 100 \text{ amperes,}$$

$$s = 10 \text{ mm} \cdot 0.81 \text{ mm} = 8.1 \text{ mm}^2, \text{ and}$$

$$\sigma = 8333.33 \text{ mho/mm.}$$

Substituting into Equation (5.7) for  $I$  and  $s$  gives

$$J_x = 12.3457 \text{ ampere/mm}^2.$$

Substituting into Equation (5.6) for  $J_x$  and  $\sigma$  gives

$$E_x = 1.4815 \cdot 10^{-3} \text{ volt/mm.}$$

The constant of integration in Equation (5.4) can be determined by applying the boundary condition

$$\phi = 10 \text{ volts @ } x = 40 \text{ mm.}$$

Rearranging Equation (5.4) gives

$$C = \phi + E_x x. \quad (5.8)$$

Substituting into Equation (5.8) for  $\phi$ ,  $E_x$ , and  $x$  gives

$$C = 10.05926 \text{ volts.}$$

Substituting into Equation (5.4) for  $E_x$  and  $C$  gives

$$\phi = [(-1.4815 \cdot 10^{-3}) x + (10.05926)] \text{ volts.} \quad (5.9)$$

Equation (5.9) can be used to determine the voltage at any point along the length of the strip. The voltage at specified locations is listed in Table 5. The voltage values determined in the mathematical analysis are identical

TABLE 5  
VOLTAGE OUTPUT FROM MATHEMATICAL ANALYSIS

Axial Location, mm	Voltage
0.0	10.05926
4.0	10.05333
8.0	10.04741
12.0	10.04148
16.0	10.03556
20.0	10.02963
24.0	10.02370
28.0	10.01778
32.0	10.01185
36.0	10.00593
40.0	10.00000

to those found in the finite element analysis.

The power generated per unit volume in each element of the finite element model was defined in Chapter IV as

$$P = E_x J_x + E_y J_y + E_z J_z . \quad (4.4)$$

For one-dimensional current flow in a conductive medium,

Equation (4.4) reduces to

$$P = E_x \cdot J_x . \quad (5.10)$$

Substituting into Equation (5.10) for  $E_x$  and  $J_x$  gives

$$P = 0.01829 \text{ Watt/mm}^3 .$$

The values for  $E_x$ ,  $J_x$ , and  $P$  determined in the mathematical analysis are identical to those found in the finite element analysis for the ten equal sized elements.

#### 5.4 Finite Element Thermal Analysis

The finite element model used for the thermal analysis is the same model which was used for the electrical analysis and is described in Section 5.2. Thermal loading came from the heat input file which is summarized in Table 4. The temperature at each end of the rectangular strip was held fixed at 23°C, causing heat to flow out the ends of the strip and creating a varying temperature field within the strip.

The MSC/NASTRAN grid point temperature output is listed in Table 6 and a plot of temperature isotherms is shown in Fig. 14.

#### 5.5 Mathematical Thermal Analysis

Steady-state heat conduction in a thermally conductive medium was defined in Chapter III as

$$\bar{\nabla} ( K \cdot \bar{\nabla} T ) = - \dot{q} . \quad (3.3)$$

For steady-state one-dimensional heat conduction in a thermally conductive medium with uniform thermal conductivity, Equation (3.3) reduces to

$$\frac{d^2 T}{dx^2} + \frac{\dot{q}}{K} = 0 , \quad (5.11)$$

where T is the temperature,

x is the axial position,

$\dot{q}$  is the heat generated per unit volume, and

K is the thermal conductivity.

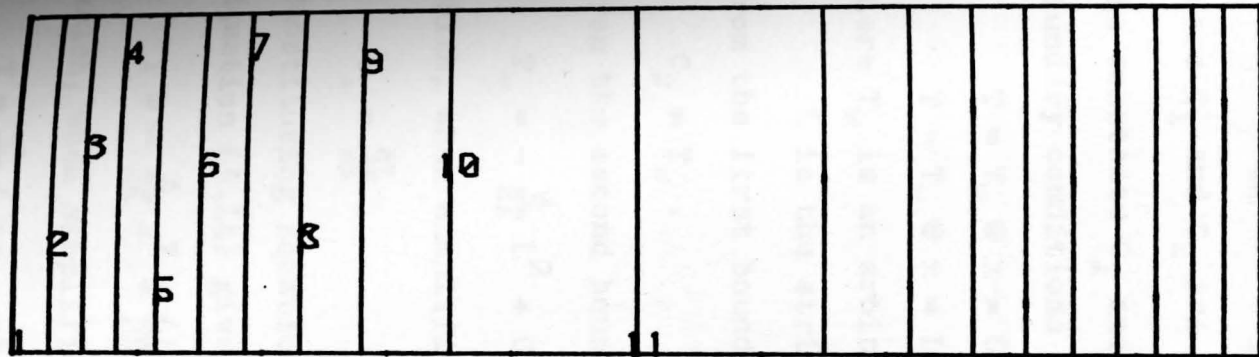
TABLE 6  
TEMPERATURE OUTPUT

Grid Point	Axial Location, mm	Temperature, °C
1	0.0	23.00
2	0.0	23.00
3	4.0	53.64
4	4.0	53.64
5	8.0	77.47
6	8.0	77.47
7	12.0	94.50
8	12.0	94.50
9	16.0	104.71
10	16.0	104.71
11	20.0	108.12
12	20.0	108.12
13	24.0	104.71
14	24.0	104.71
15	28.0	94.50
16	28.0	94.50
17	32.0	77.47
18	32.0	77.47
19	36.0	53.64
20	36.0	53.64
21	40.0	23.00
22	40.0	23.00
23	-0.0001	23.00
24	-0.0001	23.00

Rearranging Equation (5.11) gives

$$\frac{d^2 T}{dx^2} = -\frac{q}{K} \quad (5.12)$$

Separating variables in Equation (5.12) gives



<u>Symbol</u>	<u>Value<sup>a</sup></u>	<u>Symbol</u>	<u>Value<sup>a</sup></u>
1	23.00	7	74.07
2	31.51	8	82.58
3	40.02	9	91.09
4	48.53	10	99.60
5	57.05	11	108.12
6	65.56		

Fig. 14. Temperature Isotherms — Steady-State Analysis

<sup>a</sup>Temperature in °C.

$$d^2T = - \frac{q}{K} dx^2 . \quad (5.13)$$

Integrating Equation (5.13) twice gives

$$T = - \frac{q}{2K} x^2 + C_1 x + C_2 , \quad (5.14)$$

where  $C_1$  and  $C_2$  are constants of integration.

The constants  $C_1$  and  $C_2$  can be determined by applying the boundary conditions

$$T = T_w @ x = 0, \text{ and}$$

$$T = T_w @ x = L,$$

where  $T_w$  is an arbitrary fixed temperature, and

$L$  is the strip length.

From the first boundary condition,

$$C_2 = T_w . \quad (5.15)$$

From the second boundary condition,

$$T_w = - \frac{q}{2K} L^2 + C_1 L + T_w , \quad (5.16)$$

which, when simplified, gives

$$C_1 = \frac{qL}{2K} . \quad (5.17)$$

Substituting Equation (5.15) and Equation (5.17) into Equation (5.14) gives

$$T = - \frac{q}{2K} x^2 + \frac{qL}{2K} x + T_w , \quad (5.18)$$

which, when simplified, gives

$$T = \frac{q}{2K} ( Lx - x^2 ) + T_w . \quad (5.19)$$

Equation (5.19) can be used to determine the temperature at any point along the length of the strip. For the

rectangular strip described in Section 5.1,

$$L = 40 \text{ mm},$$

$$T_w = 23^\circ\text{C},$$

$$\dot{q} = 0.0183 \text{ Watt/mm}^3, \text{ and}$$

$$K = 0.043 \text{ Watt/mm-}^\circ\text{C}.$$

The temperature at specified locations along the length of the strip is listed in Table 7. The temperature values determined in the mathematical analysis are identical to those found in the finite element analysis.

TABLE 7

TEMPERATURE OUTPUT FROM MATHEMATICAL ANALYSIS

Axial Location, mm	Temperature, °C
0.0	23.00
4.0	53.64
8.0	77.47
12.0	94.50
16.0	104.71
20.0	108.12
24.0	104.71
28.0	94.50
32.0	77.47
36.0	53.64
40.0	23.00

## CHAPTER VI

## TRANSIENT ANALYSIS OF A RECTANGULAR STRIP

6.1 Introduction

The analytical procedure for a transient analysis was described in Section 4.4. The procedure is applied in this chapter to the rectangular strip described in Section 5.1. A constant electrical load of 100 amperes at 10 volts was applied to the strip so that the stabilized temperature distribution determined in the transient analysis could be compared to the steady-state temperature distribution determined in Chapter V. The electrical loading for the transient analysis is taken to be a step function as shown in Fig. 15.

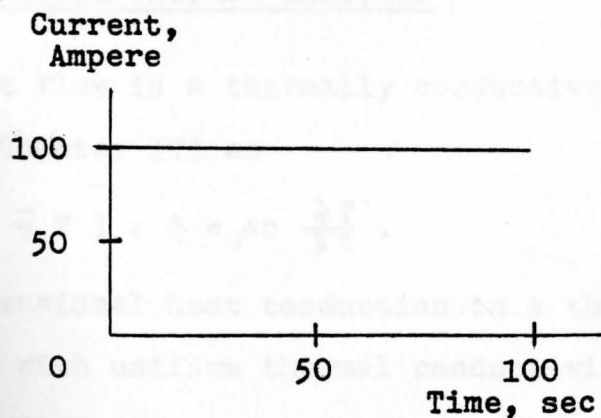


Fig. 15. Curve of Current vs. Time For Transient Analysis.



## 6.2 Finite Element Thermal Analysis

The finite element model used for the thermal analysis was the same model which was described in Section 5.2. Thermal loading for the transient analysis came from the heat input file generated in the steady-state electrical analysis described in Section 5.2. The loading was applied over a 100 second time period. Additions to the thermal program required for the transient analysis included initialized grid point temperatures ( $23^{\circ}\text{C}$ ) and the heat capacity per unit volume ( $\rho c = 0.369 \times 10^{-2} \text{ Joule/mm}^3 - ^{\circ}\text{C}$ ) for the SAE 1010 steel.

The MSC/NASTRAN transient temperature output for the 100 second time period is shown in Fig. 16. Temperatures stabilize after approximately 80 seconds, with the predicted values falling within 2% of the steady-state temperatures found in Chapter V.

## 6.3 Mathematical Thermal Analysis

Heat flow in a thermally conductive medium was defined in Chapter III as

$$\bar{\nabla} ( K \cdot \bar{\nabla} T ) + \dot{q} = \rho c \frac{\partial T}{\partial t} . \quad (3.1)$$

For one-dimensional heat conduction in a thermally conductive medium with uniform thermal conductivity, Equation (3.1) reduces to

$$\frac{\partial^2 T}{\partial x^2} + \frac{\dot{q}}{K} = \frac{1}{\alpha} \frac{\partial T}{\partial t} , \quad (6.1)$$

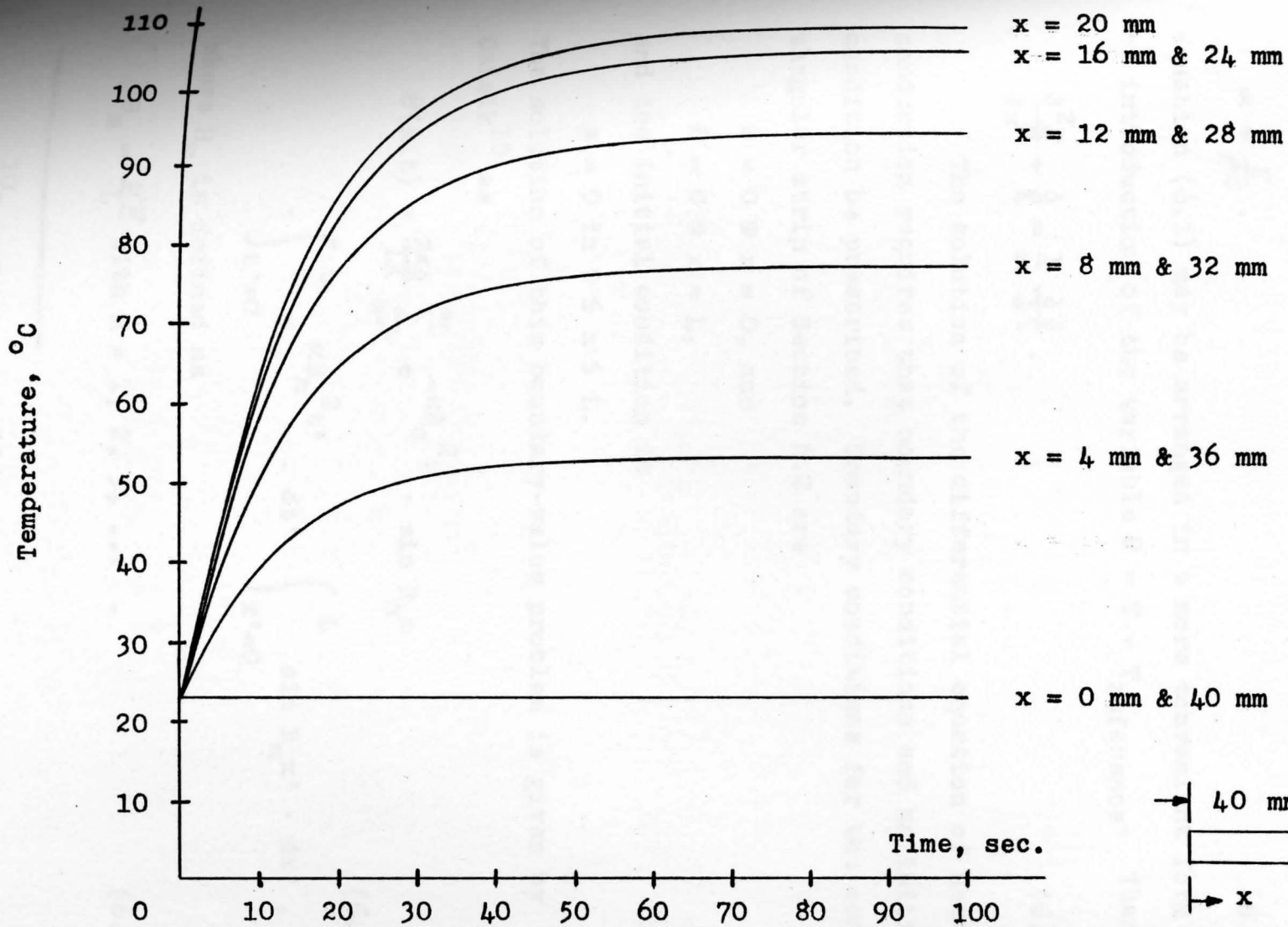


Fig. 16. Transient Temperature Output

where  $\alpha$  is the thermal diffusivity of the media and is defined as

$$\alpha = \frac{K}{\rho c} . \quad (6.2)$$

Equation (6.1) may be arranged in a more convenient form by introduction of the variable  $\theta = T - T_{\text{reference}}$ . Then

$$\frac{\partial^2 \theta}{\partial x^2} + \frac{q}{K} = \frac{1}{\alpha} \frac{\partial \theta}{\partial t} . \quad (6.3)$$

The solution of the differential equation of heat conduction requires that boundary conditions and an initial condition be prescribed. Boundary conditions for the rectangular strip of Section 6.2 are

$$\theta = 0 @ x = 0, \text{ and}$$

$$\theta = 0 @ x = L,$$

and the initial condition is

$$\theta = 0 \text{ in } 0 \leq x \leq L.$$

The solution of this boundary-value problem is given by Ozisik<sup>10</sup> as

$$\theta(x,t) = \frac{2\alpha q}{LK} \sum_{m=1}^{\infty} e^{-\alpha B_m^2 t} \cdot \sin B_m x \cdot \int_{t'=0}^t e^{\alpha B_m^2 t'} \cdot dt' \int_{x'=0}^L \sin B_m x' \cdot dx' , \quad (6.4)$$

where  $B_m$  is defined as

$$B_m = \frac{m\pi}{L} \text{ with } m = 1, 2, 3, \dots . \quad (6.5)$$

---

<sup>10</sup>Ozisik, pp. 59-66.

Performing the integration in Equation (6.4) gives

$$\int_{t'=0}^t e^{\alpha B_m^2 t'} \cdot dt' = \frac{1}{\alpha B_m^2} \left[ e^{\alpha B_m^2 t'} \right]_{t'=0}^t$$

$$= \frac{1}{\alpha B_m^2} \left[ e^{\alpha B_m^2 t} - 1 \right], \text{ and}$$
(6.6)

$$\int_{x'=0}^L \sin B_m x' \cdot dx' = \frac{1}{B_m} \left[ -\cos B_m x' \right]_{x'=0}^L$$

$$= \frac{1}{B_m} \left[ -\cos B_m L + 1 \right].$$
(6.7)

Substituting Equation (6.6) and Equation (6.7) into Equation (6.4) gives

$$\theta(x,t) = \frac{2\alpha\delta}{LK} \sum_{m=1}^{\infty} e^{-\alpha B_m^2 t} \cdot \sin B_m x$$

$$\cdot \frac{1}{\alpha B_m^2} \left[ e^{\alpha B_m^2 t} - 1 \right] \cdot \frac{1}{B_m} \left[ -\cos B_m L + 1 \right].$$
(6.8)

Rearranging Equation (6.8) gives

$$\theta(x,t) = \frac{2\delta}{LK} \sum_{m=1}^{\infty} \frac{1}{B_m^3} \cdot \sin B_m x \cdot \left[ -\cos B_m L + 1 \right]$$

$$\cdot \left[ 1 - e^{-\alpha B_m^2 t} \right].$$
(6.9)

Substituting Equation (6.5) into Equation (6.9) gives

$$\theta(x,t) = \frac{2qL^2}{K\pi^3} \sum_{m=1}^{\infty} \frac{1}{m^3} \cdot \sin \frac{m\pi x}{L} \cdot \left[ -\cos m\pi + 1 \right] \cdot \left[ 1 - e^{-\alpha \left( \frac{m\pi}{L} \right)^2 t} \right]. \quad (6.10)$$

Equation (6.10) can be used to find the thermal response at any point along the length of the strip. For the rectangular strip described in Section 6.2,

$$L = 40 \text{ mm},$$

$$q = 0.0183 \text{ Watt/mm}^3,$$

$$K = 0.043 \text{ Watt/mm-}^\circ\text{C}, \text{ and}$$

$$\alpha = 11.6531 \text{ mm}^2/\text{sec}.$$

The thermal response at the center of the strip ( $x = 20 \text{ mm}$ ) is listed in Table 8. Also listed are the corresponding temperature values from the finite element analysis. The mathematical analysis predicts a more rapid build-up of temperature than does the finite element analysis. In both cases, the temperature stabilizes at  $85^\circ\text{C}$  above ambient. The error in the finite element solution (2.7% at  $t = 20$  seconds) can be attributed to the fact that the algorithm used to integrate Equation (6.1) is a compromise between stability, efficiency and accuracy.

TABLE 8  
 MATHEMATICAL VS. FINITE ELEMENT RESULTS  
 FOR  $x = 20$  mm

Time, sec	Temperature <sup>a</sup> , °C	
	Mathematical	Finite Element
0	0.0	0.0
20	64.30	62.58
40	80.20	79.46
60	83.98	83.60
80	84.88	84.66
100	85.09	84.95

<sup>a</sup>Temperature above ambient.

## CHAPTER VII

### STEADY-STATE ANALYSIS OF A RECTANGULAR STRIP WITH TEMPERATURE-DEPENDENT MATERIAL PROPERTIES

#### 7.1 Introduction

The analytical procedure for a steady-state analysis with temperature-dependent material properties was described in Section 4.5. The procedure is applied in this chapter to the rectangular strip described in Section 5.1. Curves of electrical conductivity and thermal conductivity versus temperature for SAE 1010 steel are shown in Fig. 28 and Fig. 29 of the Appendix.

The finite element model used for both the electrical and thermal analyses was the same model which was described in Section 5.2. Electrical loading for the electrical analysis was 100 amperes at 10 volts. For the thermal analysis, the temperature at each end of the rectangular strip was held fixed at 23°C. These loading and boundary conditions held for each of the iterative steady-state solutions.

#### 7.2 Analytical Results

The electrical conductivity used for each iteration is listed in Table 9. For the first iteration, a constant value of electrical conductivity based on the ambient

TABLE 9  
ELECTRICAL CONDUCTIVITY PER ITERATION

Element	Electrical Conductivity, mho/mm				
	Iteration 1	Iteration 2	Iteration 3	Iteration 4	Iteration 5
1	8333	7000	6800	6700	6700
2	8333	6000	5500	5400	5400
3	8333	5500	5200	5000	5000
4	8333	5400	4800	4700	4700
5	8333	5300	4700	4500	4500
6	8333	5300	4700	4500	4500
7	8333	5400	4800	4700	4700
8	8333	5500	5200	5000	5000
9	8333	6000	5500	5400	5400
10	8333	7000	6800	6700	6700
11	8333	7000	6800	6700	6700



temperature ( $23^{\circ}\text{C}$ ) was used. Thereafter, the electrical conductivity for each element was based on the average element temperature from the previous iteration. As shown in Table 9, the solution converged after five iterations.

The MSC/NASTRAN grid point temperature output for each iteration is listed in Table 10 and the maximum temperature for each iteration is listed in Table 11. The maximum temperature for the converged solution is 80% higher than that obtained from the steady-state analysis neglecting temperature-dependent material properties.

TABLE 10

## ITERATIVE TEMPERATURE OUTPUT

Grid Point	Axial Location, mm	Temperature, °C				
		Iteration 1	Iteration 2	Iteration 3	Iteration 4	Iteration 5
1	0.0	23.00	23.00	23.00	23.00	23.00
2	0.0	23.00	23.00	23.00	23.00	23.00
3	4.0	76.64	91.02	95.26	96.73	96.73
4	4.0	76.64	91.02	95.26	96.73	96.73
5	8.0	100.47	127.40	135.45	138.29	138.29
6	8.0	100.47	127.40	135.45	138.29	138.29
7	12.0	117.56	154.19	165.38	169.28	169.28
8	12.0	117.56	154.19	165.38	169.28	169.28
9	16.0	127.86	170.54	183.88	188.50	188.50
10	16.0	127.86	170.54	183.88	188.50	188.50
11	20.0	131.31	176.06	190.11	195.03	195.03
12	20.0	131.31	176.06	190.11	195.03	195.03
13	24.0	127.86	170.54	183.88	188.50	188.50
14	24.0	127.86	170.54	183.88	188.50	188.50
15	28.0	117.56	154.19	165.38	169.28	169.28
16	28.0	117.56	154.19	165.38	169.28	169.28
17	32.0	100.47	127.40	135.45	138.29	138.29
18	32.0	100.47	127.40	135.45	138.29	138.29
19	36.0	76.64	91.02	95.26	96.73	96.73
20	36.0	76.64	91.02	95.26	96.73	96.73
21	40.0	23.00	23.00	23.00	23.00	23.00
22	40.0	23.00	23.00	23.00	23.00	23.00
23	-0.0001	23.00	23.00	23.00	23.00	23.00
24	-0.0001	23.00	23.00	23.00	23.00	23.00

TABLE 11  
 MAXIMUM TEMPERATURE PER ITERATION

Iteration	Maximum Temperature <sup>a</sup> , °C
1	131.31
2	176.06
3	190.11
4	195.03
5	195.03

<sup>a</sup>Maximum temperature location is  $\frac{1}{2}$  strip length.

## CHAPTER VIII

### STEADY-STATE ANALYSIS OF A FUSIBLE TERMINAL

#### 8.1 Introduction

The analytical procedure for a steady-state analysis was described in Section 4.3. The procedure is applied in this chapter to the fusible terminal pictured in Fig. 1. The fusible terminal was analyzed in order to demonstrate the analytical procedure on a large scale problem. Loading and boundary conditions for the electrical and thermal analyses came from an experimental temperature survey where steady-state current, voltage and temperature were measured.

The fusible terminal is a SAE 1010 steel stamping. Material thickness is 0.81 mm. One end of the terminal contains a hole through which a 9.525 mm diameter mounting stud passes while the opposite end contains crimp wings for the attachment of 12 gage electrical cable. Material for the mounting stud and cable are SAE CA510 phosphor bronze and SAE CA122 copper, respectively.

#### 8.2 Experimental Temperature Survey

An experimental temperature survey was performed to provide realistic boundary and loading conditions for the electrical and thermal analyses and also to verify the

finite element results of the steady-state thermal analysis of the fusible terminal.

The experimental procedure involved applying an electrical load to the fusible terminal through a 12 volt lead-acid battery and recording the steady-state current through the test circuit, the battery voltage and the temperature adjacent to and at the fusible terminal. The temperature measurement locations are shown in Fig. 17. Location  $T_1$  is on top of the mounting stud,  $T_2$  and  $T_3$  are on the fusible terminal, and  $T_4$  is on the electrical cable, 25.4 mm from the end of the terminal.

The experimental test setup is shown schematically in Fig. 18. The fusible terminal was connected to a 12 volt lead-acid battery through 20 meters of 12 gage electrical cable and 3.5 meters of 00 gage battery cable. The 20 meters of 12 gage electrical cable was utilized to add enough resistance to the circuit so that the current flow would be low enough to prevent the melting of the fusible terminal.

Temperature measurements were taken with four 28 gage iron-constantan thermocouples. An Ewald Instrument Corp., Model PW848, welder was used to attach the thermocouples to the mounting stud, fusible terminal and cable. The thermocouple leads were attached to a rotary switch which in turn was attached to a digital temperature indicator. The rotary switch allowed the hook-up of any one

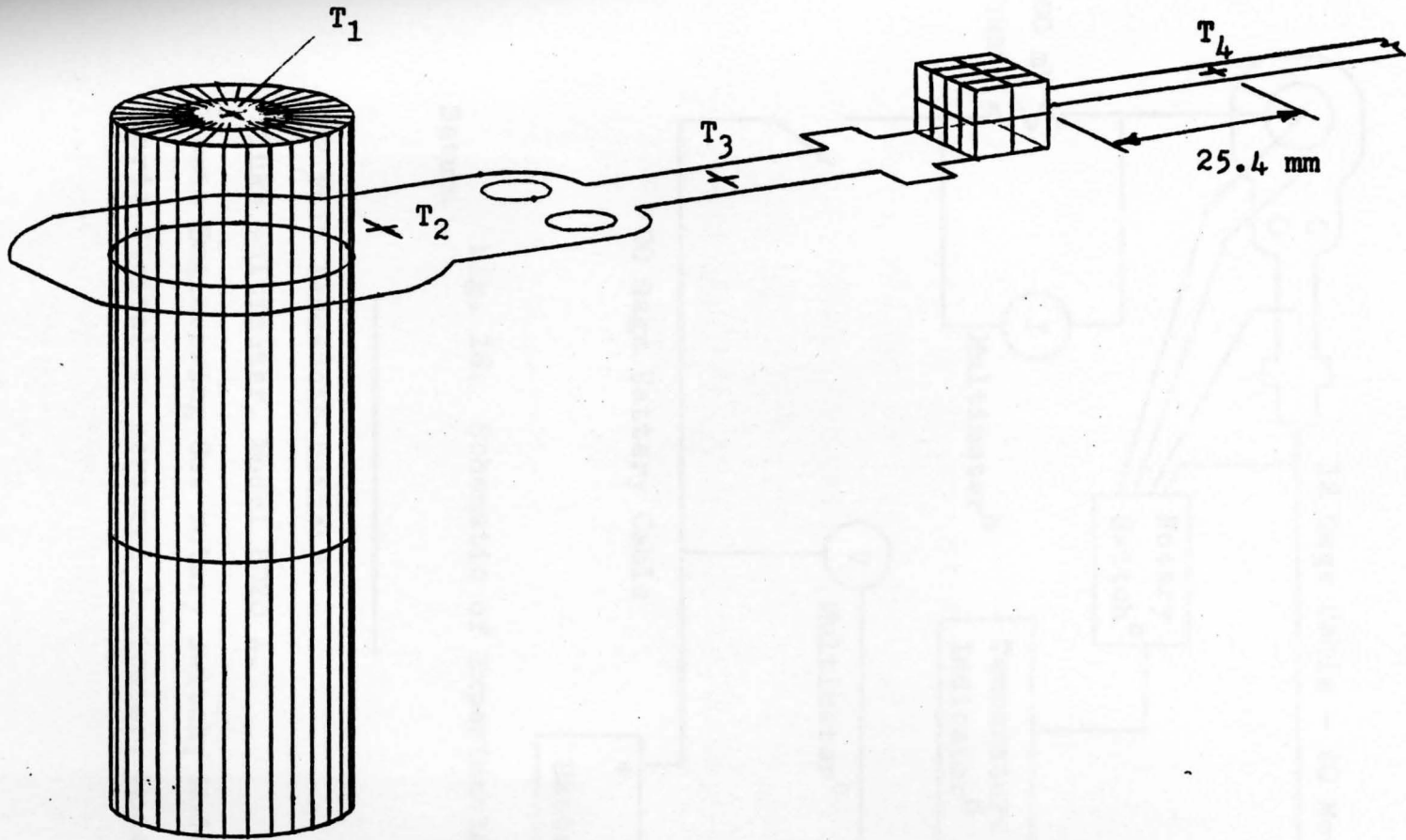


Fig. 17. Temperature Measurement Locations

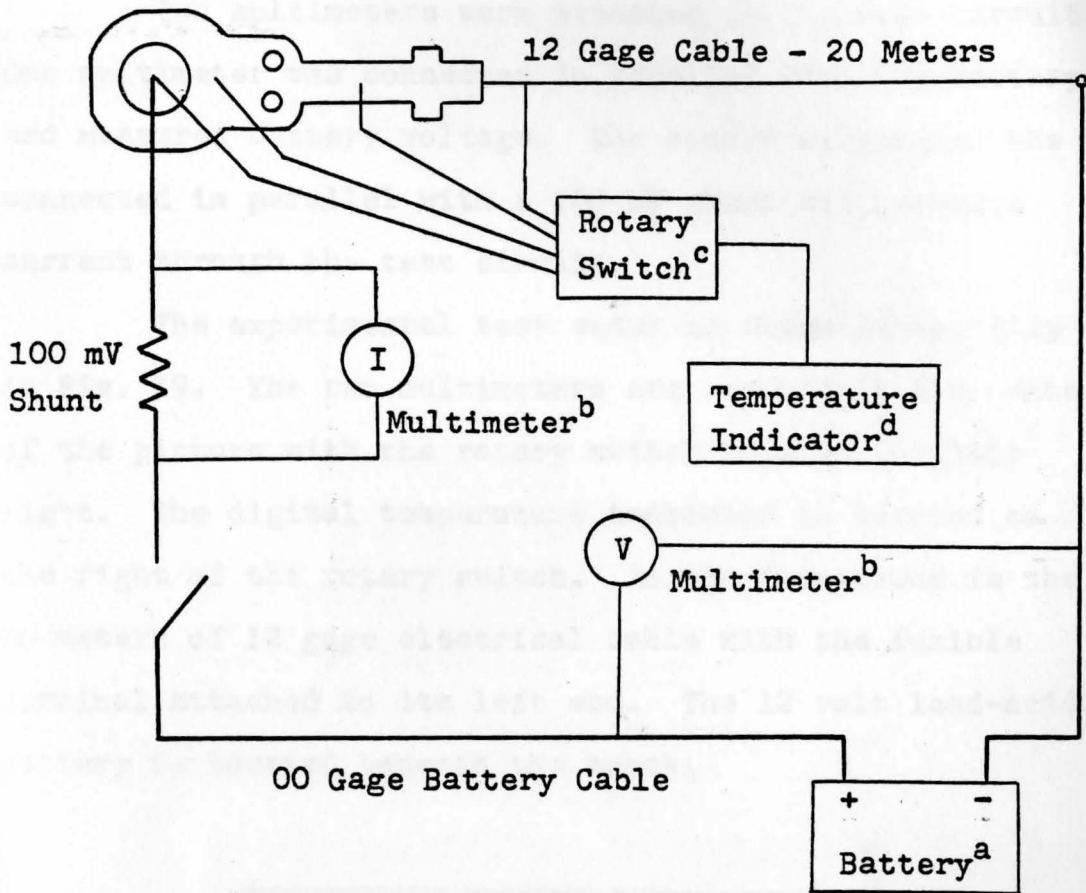


Fig. 18. Schematic of Experimental Test Setup.

<sup>a</sup>12 volt lead-acid battery.

<sup>b</sup>Fluke multimeter, Model 8020 A.

<sup>c</sup>Lewis Engineering Co. rotary switch, Model 38S2C.

<sup>d</sup>Doric digital temperature indicator, Model DS 500.

of the four thermocouple leads to the digital temperature indicator.

Two multimeters were attached to the test circuit. One multimeter was connected in parallel with the battery and measured battery voltage. The second multimeter was connected in parallel with a 100 mV shunt and measured current through the test circuit.

The experimental test setup is shown pictorially in Fig. 19. The two multimeters are located in the center of the picture with the rotary switch located to their right. The digital temperature indicator is located to the right of the rotary switch. In the foreground is the 20 meters of 12 gage electrical cable with the fusible terminal attached to its left end. The 12 volt lead-acid battery is located beneath the bench.



Fig. 19. Experimental Test Setup



Steady-state current through the test circuit, battery voltage, and mounting stud, fusible terminal and cable temperatures were obtained using the following experimental procedure:

- Step 1. Initial battery voltage was recorded.
- Step 2. Ambient temperature at location  $T_3$  was recorded.
- Step 3. The switch was closed and the temperature at location  $T_3$  was allowed to stabilize.
- Step 4. Temperatures at locations  $T_1$ ,  $T_2$ ,  $T_3$  and  $T_4$  were recorded.
- Step 5. The current through the test circuit and the battery voltage were recorded.
- Step 6. The switch was opened and the temperature at location  $T_3$  was allowed to return to the ambient temperature.

The experimental procedure was repeated until four groups of readings were obtained. Experimental results are summarized in Table 12.

### 8.3 Finite Element Electrical Analysis

The finite element model used for both the electrical and thermal analyses is shown in Fig. 20 and Fig. 21. The model consists of a 30 mm long SAE CA510 phosphor bronze mounting stud, the SAE 1010 steel fusible terminal and a 25.4 mm section of SAE CA122 copper electrical cable.

Both solid and plate elements were used to define the finite element model. Five-sided and six-sided solid

TABLE 12  
RESULTS OF EXPERIMENTAL TEMPERATURE SURVEY

Run	Initial Voltage	Current, Ampere	Steady-State Voltage	Temperature <sup>a</sup> , °C				
				T <sub>amb</sub>	T <sub>1</sub>	T <sub>2</sub>	T <sub>3</sub>	T <sub>4</sub>
1	12.71	90	10.98	23	34	83	296	166
2	12.76	86	11.04	23	39	88	294	160
3	12.73	87	11.07	23	34	85	298	109
4	12.74	88	10.88	23	33	86	300	134
Average	12.74	87.8	10.99	23	35	85.5	297	142.3

<sup>a</sup>See Fig. 17 for temperature locations.

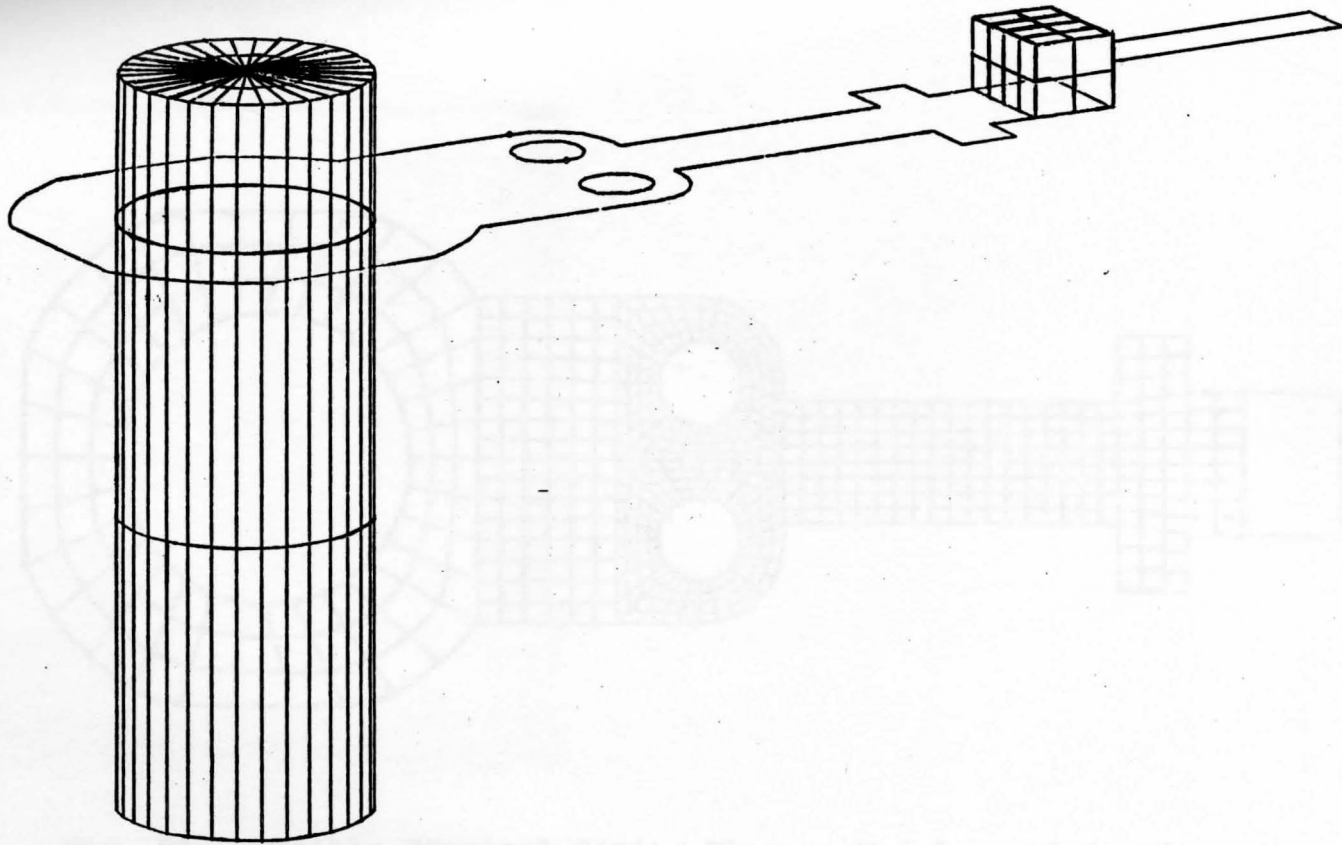


**Fig. 20. Fusible Terminal Finite Element Model — Solid Elements**

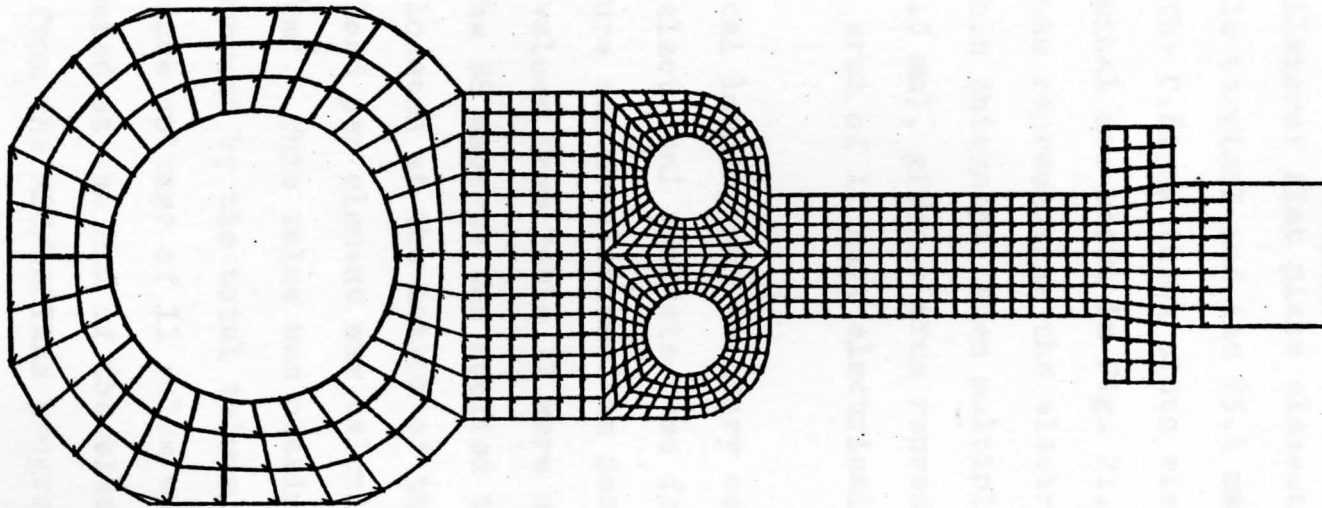


Fig. 21. Fusible Terminal Finite Element Model — Plate Elements

elements were used to model the mounting stud while six-sided solid elements were used to model the crimp area of the fusible terminal. These solid elements are shown in Fig. 20. Quadrilateral flat plate elements were used to model the fusible terminal and the 25.4 mm section of electrical cable. The 0.81 mm thick plate elements representing the fusible terminal are shown in Fig. 21. The thickness of the plate elements representing the electrical cable was set at 1.209 mm. This thickness, when multiplied by the width of the cable (2.5 mm), gives a true representation of the cross-sectional area of 12 gage electrical cable ( $3.022 \text{ mm}^2$ ).

Electrical loading and boundary conditions for the finite element electrical analysis came from the experimental temperature survey discussed in Section 8.2. The average of the values from Table 12 were used - 88 amperes at 11 volts. The 88 amperes was applied to the 32 five-sided elements located at the bottom of the mounting stud. The electrical load per element was calculated to be  $0.34865 \text{ ampere/mm}^3$ . This value was obtained by dividing the 88 ampere current by the total volume of the 32 elements. A reference voltage of 11 volts was applied to the grid points located at the end of the electrical cable.

Output from the MSC/NASTRAN program included the grid point voltages, and the electric field intensity and current density at each element of the finite element model.

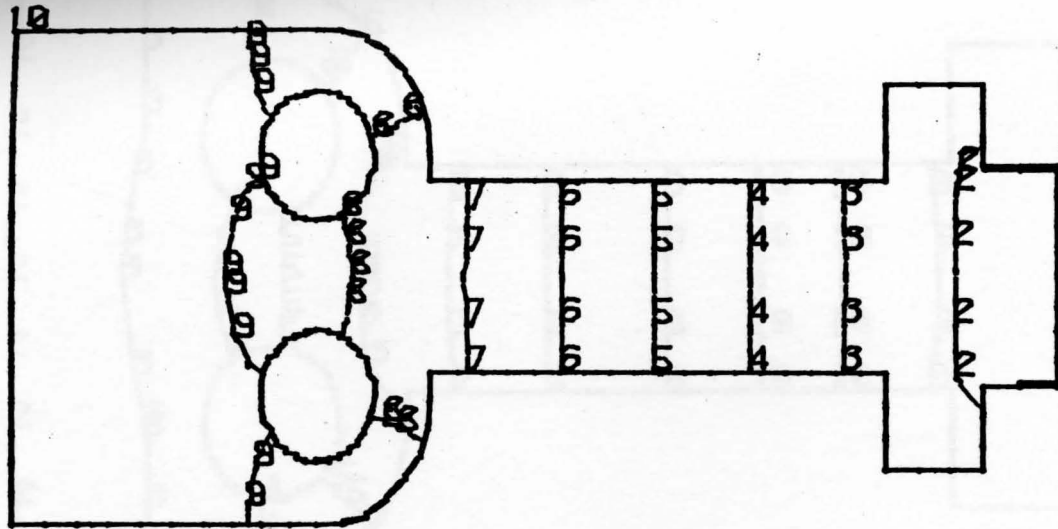
A plot of equipotential lines for a portion of the fusible terminal is shown in Fig. 22.

#### 8.4 Finite Element Thermal Analysis

The finite element model used for the thermal analysis is the same model which was used for the electrical analysis and is described in Section 8.3. Thermal loading came from the heat input file which was generated by the intermediate Fortran program after the execution of the electrical analysis. Boundary conditions for the finite element thermal analysis came from the experimental temperature survey discussed in Section 8.2. The temperature at the end of the cable was held fixed at  $142^{\circ}\text{C}$ . This value is the average of the values at location  $T_4$  from Table 12. The temperature at the bottom of the mounting stud was held fixed at  $23^{\circ}\text{C}$  since there was no temperature rise in this area during the experimental temperature survey.

Output from the MSC/NASTRAN program included the grid point temperatures, and the temperature gradient and heat flux at each element in the finite element model. A plot of temperature isotherms for a portion of the fusible terminal is shown in Fig. 23 and temperature output for selected grid points is listed in Table 13. The locations of the grid points listed in Table 13 are shown in Fig. 24 and Fig. 25.

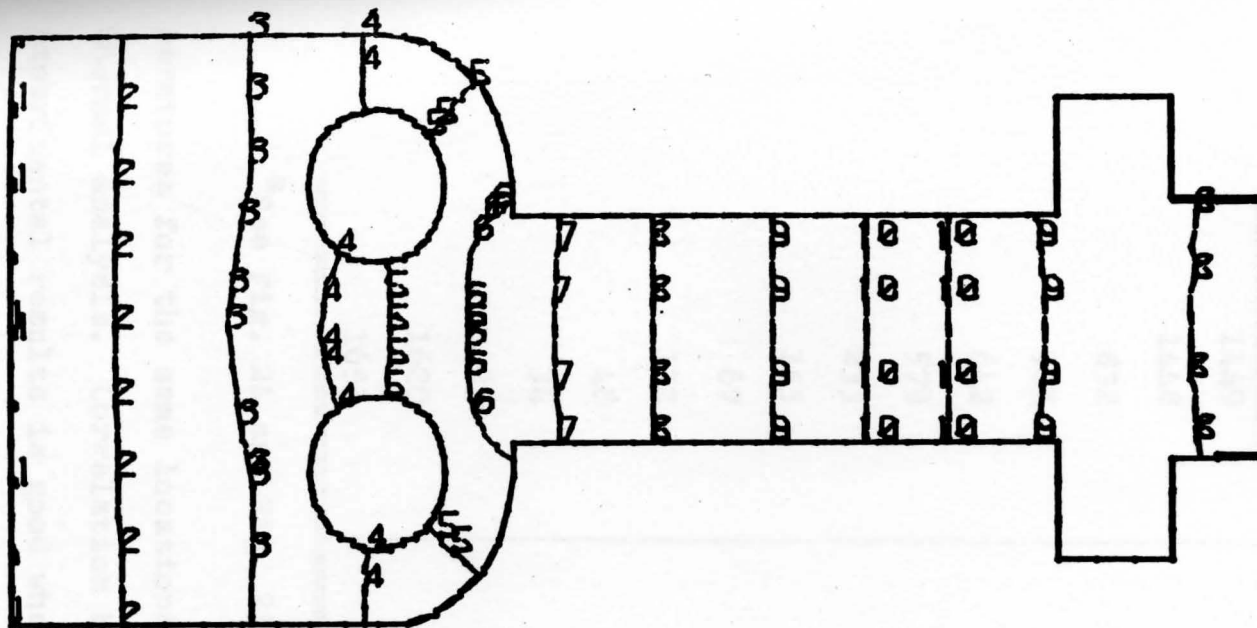
Listed in Table 14 are the average of the experimental temperatures from Table 12 and the analytical tem-



<u>Symbol</u>	<u>Value<sup>a</sup></u>	<u>Symbol</u>	<u>Value<sup>a</sup></u>
1	11.016	6	11.053
2	11.023	7	11.061
3	11.031	8	11.068
4	11.038	9	11.076
5	11.046	10	11.083

Fig. 22. Equipotential Lines — Fusible Terminal

<sup>a</sup>Electric potential in volts.



<u>Symbol</u>	<u>Value<sup>a</sup></u>	<u>Symbol</u>	<u>Value<sup>a</sup></u>
1	50.0	6	175.0
2	75.0	7	200.0
3	100.0	8	225.0
4	125.0	9	245.0
5	150.0	10	252.0

Fig. 23. Temperature Isotherms — Fusible Terminal

<sup>a</sup>Temperature in °C.



TABLE 13  
TEMPERATURE OUTPUT

Grid Point <sup>a</sup>	Temperature, °C
1449	23.00
1448	37.86
832	44.20
961	45.34
642	47.22
579	48.67
233	102.36
153	145.31
67	188.14
112	246.41
48	243.71
34	228.27
25	207.54
1620	204.37
1653	142.00

<sup>a</sup>See Fig. 24 and Fig. 25 for grid point locations.

peratures for the same locations from the finite element thermal analysis. Correlation between the analytical and experimental results is good when the assumptions made in the analytical solution are considered. The assumptions made were constant electrical and thermal conductivities and no convective or radiative heat losses.

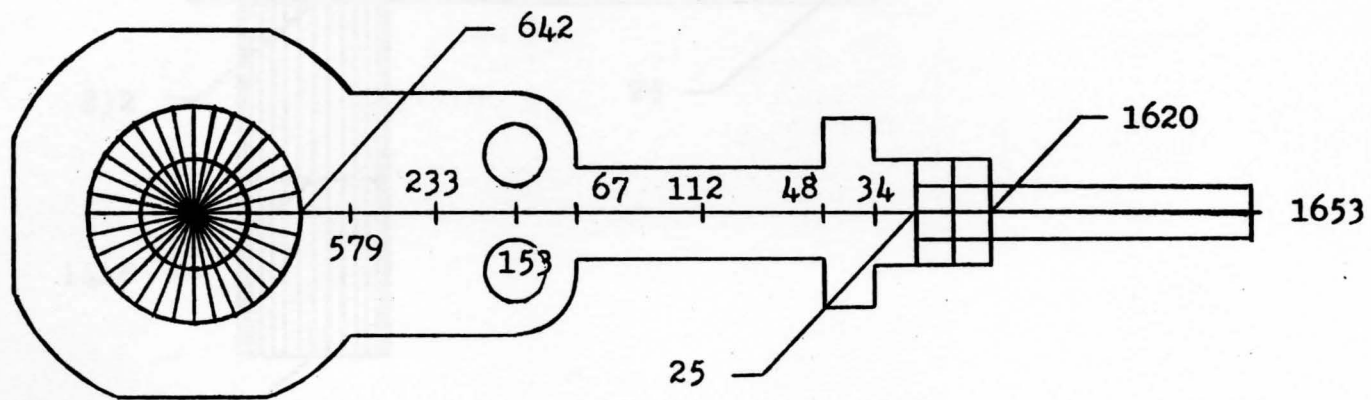


Fig. 24. Grid Point Locations For Thermal Output

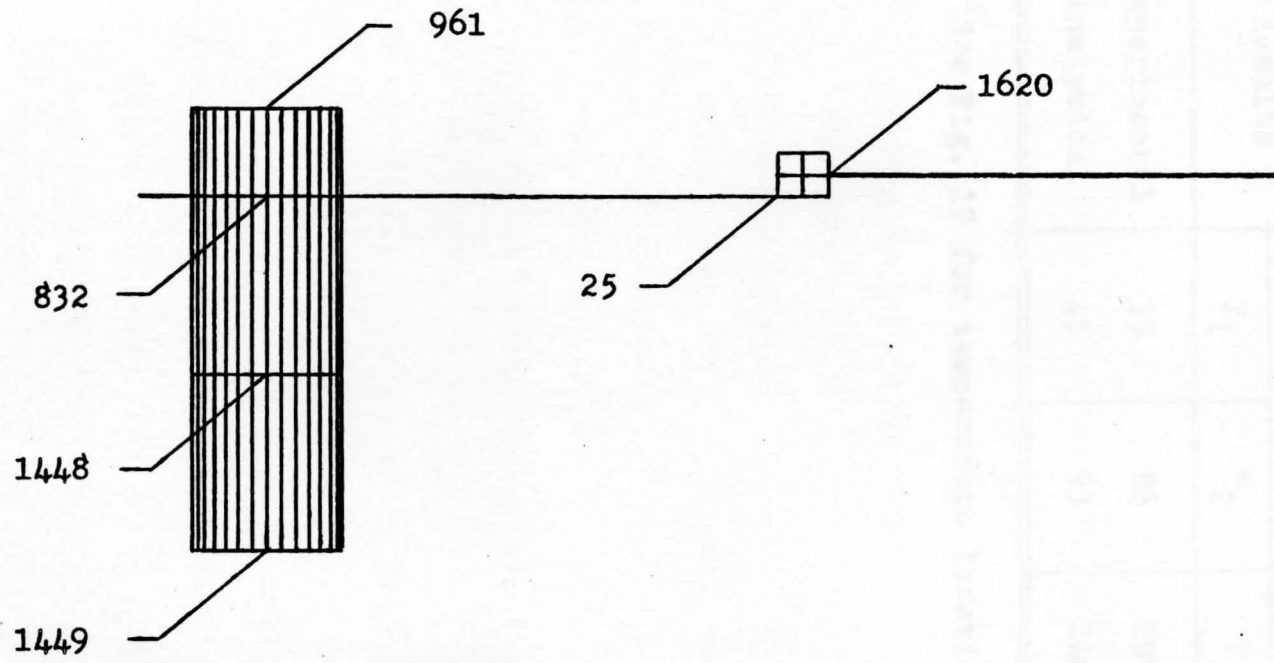


Fig. 25. Grid Point Locations For Thermal Output

TABLE 14  
EXPERIMENTAL VS. ANALYTICAL RESULTS

Results	Temperature <sup>a</sup> , °C			
	T <sub>1</sub>	T <sub>2</sub>	T <sub>3</sub>	T <sub>4</sub>
Experimental	35	86	297	142
Analytical	45	93	246	142

<sup>a</sup>See Fig. 17 for temperature locations.

## CHAPTER IX

## CONCLUSIONS AND DISCUSSION

9.1 Conclusions

The analytical procedure for evaluating the thermal response of a conductive medium subjected to electrical loading has been demonstrated on a simple flat plate structure and a complex structure representing a fusible terminal. These demonstrations have shown the procedure to be a valid and a versatile one.

The validity of the analytical procedure has been established through mathematical analysis. The finite element steady-state and transient solutions of the rectangular strip show excellent correlation with the corresponding mathematical solutions.

The versatility of the analytical procedure is a result of the versatility of the finite element technique itself. The ability to realistically model any geometric configuration, the ability to determine the steady-state and transient response, and the ability to incorporate temperature-dependent material properties are just a few of the features which make the finite element technique a highly versatile design tool.

The need to incorporate temperature-dependent material properties into the solution sequence was demonstrated

in Chapter VII. However, the process of manually iterating until the solution converges makes this approach unrealistic for a large-scale problem such as the fusible terminal. Also, the manual iteration scheme applies only to a steady-state solution. An alternative to this manual iteration scheme must be developed in order to overcome these shortcomings of the analytical procedure.

The inability to accept a varying electrical load is another shortcoming of the analytical procedure. This shortcoming must also be overcome since a constant electrical load is very seldom found in a design application. A typical curve of current versus time for a fusible terminal protecting three meters of 12 gage electrical cable in a short circuit condition is shown in Fig. 26.

## 9.2 Discussion

The shortcomings of the analytical procedure for evaluating the thermal response of a conductive medium subjected to electrical loading were discussed in Section 9.1. These were the manual iteration scheme for the incorporation of temperature-dependent material properties and the inability to accept varying electrical load. The proposed analytical procedure for eliminating these shortcomings is shown in Fig. 27.

The analytical procedure utilizes a time step solution technique. An electrical load such as that shown in Fig. 26 is applied in an incremental fashion. For each time

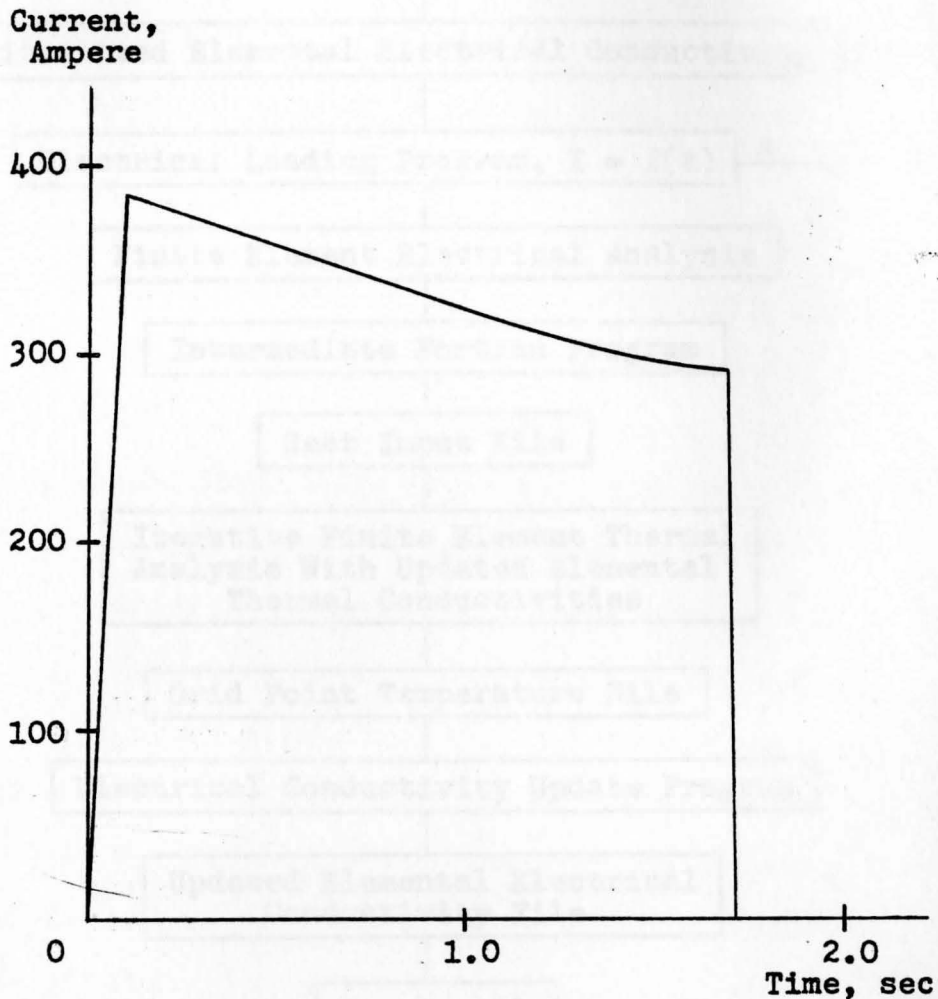


Fig. 26. Curve of Current vs. Time For Fusible Terminal Protecting Three Meters of 12 Gage Cable.

interval, a finite element electrical and thermal solution is obtained. The thermal solution automatically accounts for the thermal conductivity change with temperature. Grid point temperatures are output from the thermal analysis and are used by an electrical conductivity update program to update the electrical conductivity for each element of the finite element model. Time is incremented and a new elec-

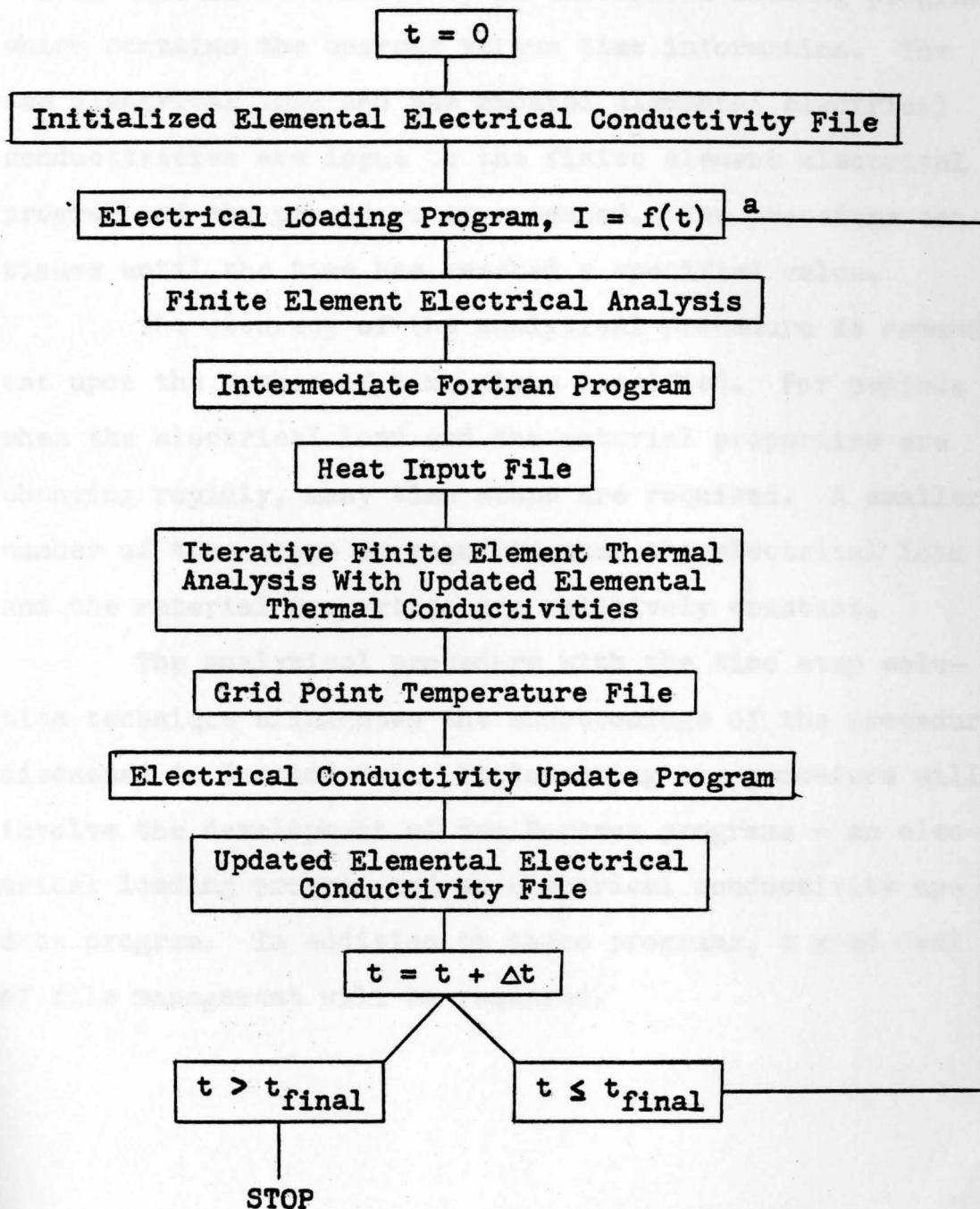


Fig. 27. Flow Diagram of Analytical Procedure With Automated Time Step Solution Technique.

<sup>a</sup> $I = f(t)$  from Fig. 26.



trical load is determined by an electrical loading program which contains the current versus time information. The new electrical load and the updated elemental electrical conductivities are input to the finite element electrical program and the procedure is repeated. The procedure continues until the time has reached a specified value.

The accuracy of the analytical procedure is dependent upon the number of time steps specified. For periods when the electrical load and the material properties are changing rapidly, many time steps are required. A smaller number of time steps is required when the electrical load and the material properties are relatively constant.

The analytical procedure with the time step solution technique eliminates the shortcomings of the procedure discussed in Section 9.1. Implementing the procedure will involve the development of two Fortran programs - an electrical loading program and an electrical conductivity update program. In addition to these programs, a good deal of file management will be required.

## APPENDIX

Material Properties

TABLE 14

MATERIAL PROPERTIES<sup>a</sup>

Property (Units)	SAE 1010 Steel	SAE 4140 Steel	SAE 4340 Steel	SAE 52100 Steel	SAE 6150 Steel	SAE 6150 Steel	SAE 6150 Steel
Thermal Conductivity, $k$ (Watts/m <sup>2</sup> · °C)	0.043	0.043	0.043	0.043	0.043	0.043	0.043
Density, $\rho$ (lb/in <sup>3</sup> )	$7.87 \times 10^{-6}$	$7.87 \times 10^{-6}$	$7.87 \times 10^{-6}$	$7.87 \times 10^{-6}$	$7.87 \times 10^{-6}$	$7.87 \times 10^{-6}$	$7.87 \times 10^{-6}$
Electrical Conductivity, $\sigma$ (ohm <sup>-1</sup> · in)	0.0113	0.0113	0.0113	0.0113	0.0113	0.0113	0.0113
Heat Capacity per Unit Volume, $c_v$ (Btu/in <sup>3</sup> · °F)	$0.119 \times 10^{-2}$	$0.119 \times 10^{-2}$	$0.119 \times 10^{-2}$	$0.119 \times 10^{-2}$	$0.119 \times 10^{-2}$	$0.119 \times 10^{-2}$	$0.119 \times 10^{-2}$

<sup>a</sup> Properties at 20°C.

TABLE 15

MATERIAL PROPERTIES<sup>a</sup>

Property (Unit)	Material		
	SAE 1010 Steel	SAE CA122 Copper	SAE CA510 Phosphor Bronze
Thermal Conductivity, K (Watt/mm - °C)	0.043	0.339	0.069
Density, $\rho$ (kg/mm <sup>3</sup> )	$7.87 \times 10^{-6}$	$8.94 \times 10^{-6}$	$8.86 \times 10^{-6}$
Electrical Conductivity, $\sigma$ (mho/mm)	8333.3	49261.1	8695.7
Heat Capacity Per Unit Volume, $\rho c$ (Joule/mm <sup>3</sup> - °C)	$0.369 \times 10^{-2}$	$0.343 \times 10^{-2}$	$0.336 \times 10^{-2}$

<sup>a</sup>Properties at 20°C.

Electrical Conductivity,  
mho/mm

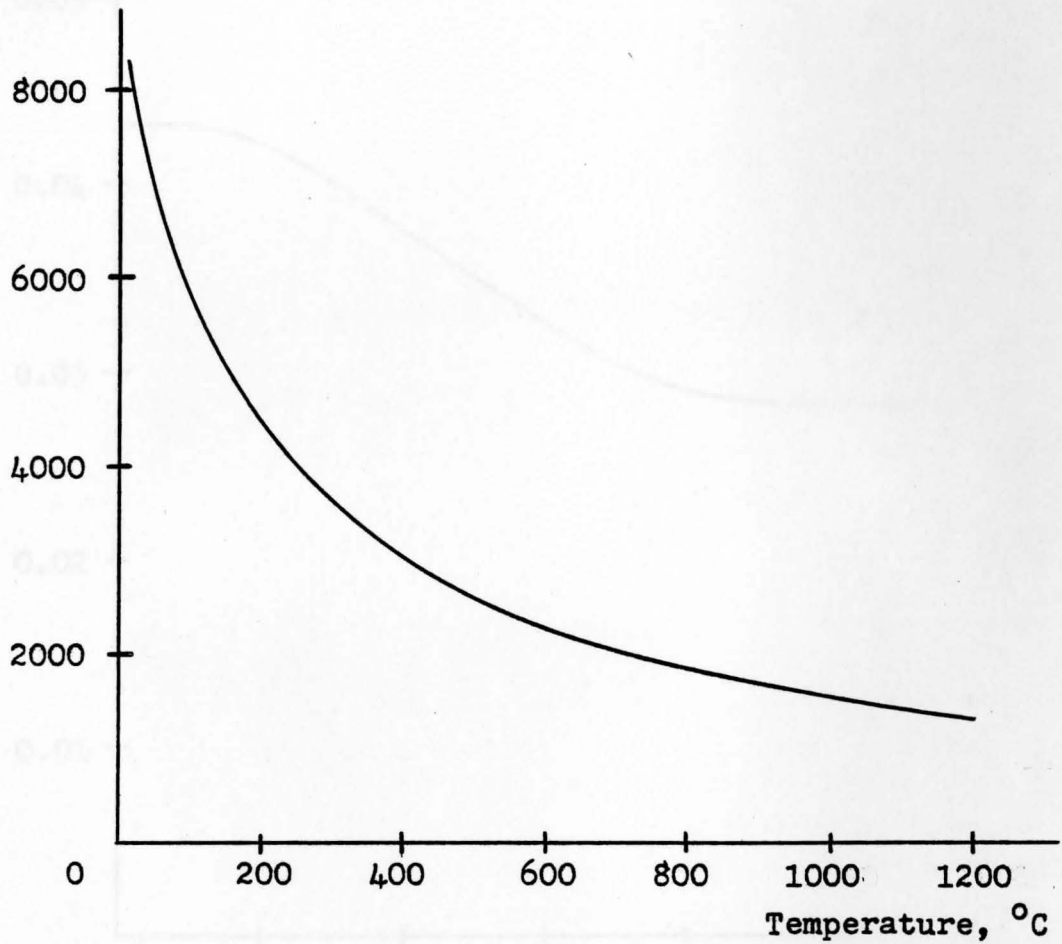


Fig. 28. Curve of Electrical Conductivity vs. Temperature For SAE 1010 Steel.

Thermal Conductivity,  
Watt/mm - °C

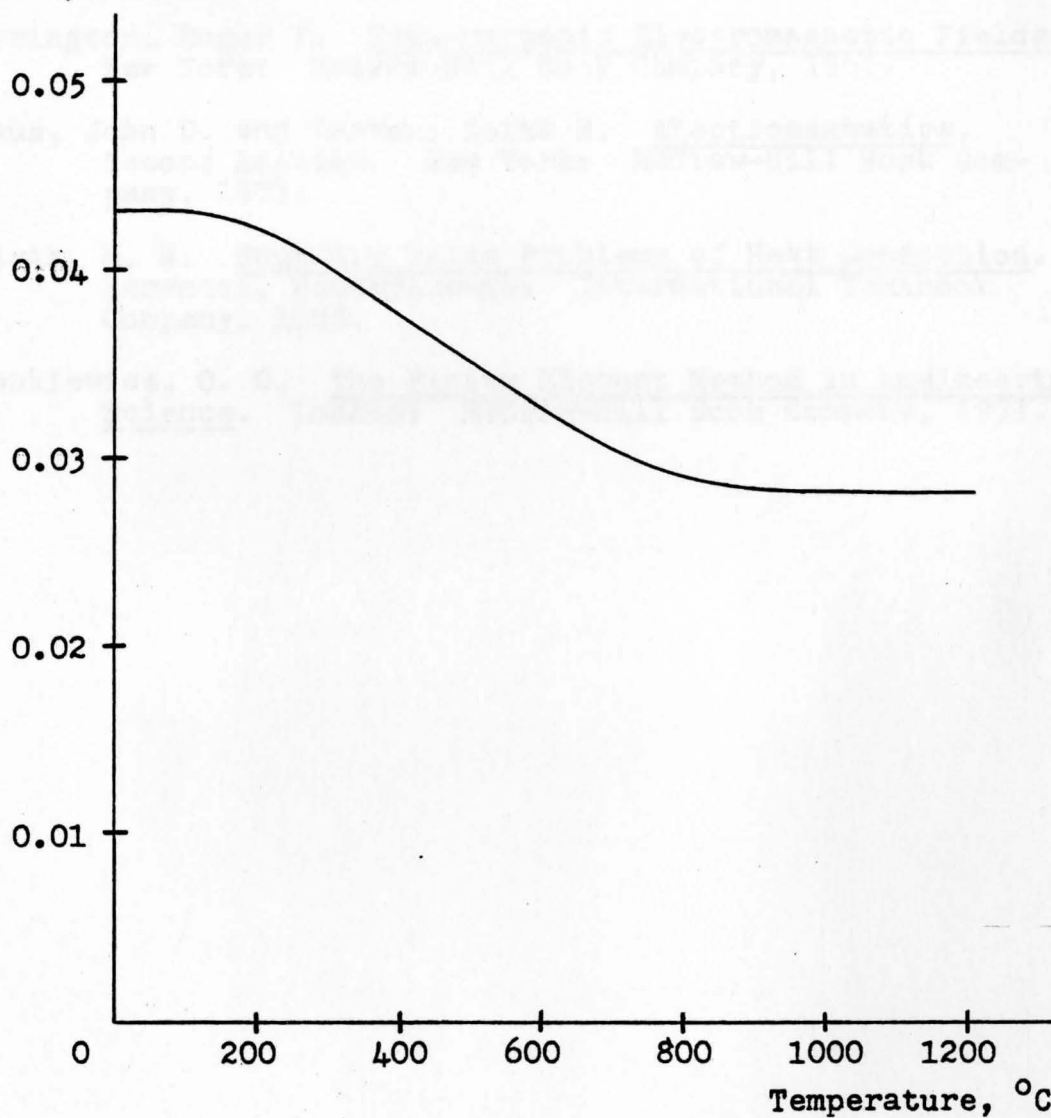


Fig. 29. Curve of Thermal Conductivity vs. Temperature For SAE 1010 Steel.

## BIBLIOGRAPHY

- Brauer, John R. "MSC/NASTRAN Analysis of Electric Currents in Cathodic Protection Systems." Proceedings of the MSC/NASTRAN Users Conference. Pasadena, California, March, 1979.
- Harrington, Roger F. Time-Harmonic Electromagnetic Fields. New York: McGraw-Hill Book Company, 1961.
- Kraus, John D. and Carver, Keith R. Electromagnetics, Second Edition. New York: McGraw-Hill Book Company, 1973.
- Ozsisik, M. N. Boundary Value Problems of Heat Conduction. Scranton, Pennsylvania: International Textbook Company, 1968.
- Zienkiewicz, O. C. The Finite Element Method in Engineering Science. London: McGraw-Hill Book Company, 1971.

## REFERENCES

- Holman, J. P. Heat Transfer, Third Edition. New York: McGraw-Hill, 1972.
- Keribar, Rifat and Shang, J. C. "Overview of MSC/NASTRAN Heat Transfer Capabilities." Proceedings of the Conference on Finite Element Methods and Technology. Pasadena, California, March 1981.
- MSC/NASTRAN Users Manual. MacNeal-Schwendler Corporation, 1978, Volume I, Section 1.8.
- Seegerlind, Larry J. Applied Finite Element Analysis. New York: John Wiley and Sons, 1976.
- The NASTRAN Theoretical Manual. MacNeal-Schwendler Corporation, 1972, Section 8.